AD744084

RADC-TR-72-68
Final Technical Report
March 1972

DIAL PACK DUST CLOUD DATA ANALYSIS

Contractor: Spectran, Incorporated
Contract Number: F30602-71-C-0297
Effective Date of Contract: 26 May 1971
Contract Expiration Date: 15 January 1971
Amount of Contract: $24,109.00

Principal Investigator: J. C. Auckland
Phone: 213 469-7343

Project Engineer: Moses A. Diab
Phone: 315 330-2847

Sponsored by
U. S. Army Advanced Ballistic Missile Defense Agency
Army MIPR No. A31699-13-Z575

Approved for public release;
distribution unlimited.

Rome Air Development Center
Air Force Systems Command
Griffiss Air Force Base, New York

Reproduced by
NATIONAL TECHNICAL
INFORMATION SERVICE
U S Department of Commerce
Springfield VA 22151

DEPARTMENT OF THE AIR FORCE
HEADQUARTERS ROME AIR DEVELOPMENT CENTER (AFSC)
GRIFFISS AIR FORCE BASE, NEW YORK 13440

REPLY TO ATTN OF: TDR/D. Engel/4204

27 March 1972

SUBJECT: TR-72-68 "Dial Pack Dust Cloud Data Analysis"

TO:
DDC/Air Force Liaison Representative
Cameron Station
Alexandria VA 22314

1. I certify that the subject TR has been reviewed and approved for public release by the controlling office and the information office in accordance with AFR 80-45/AFSC Sup 1. It may be made available or sold to the general public and foreign nationals.

2. Distribution statement A appears on the subject TR and the DD Form 1473 as required by AFRs 80-44 and 80-45.

FOR THE COMMANDER

FRED S. DYER
STINFO, RADC
Tech Data & Info Division

Atch

A

UNCLASSIFIED

Security Classification

DOCUMENT CONTROL DATA - R & D

(Security classification of title, body of abstract and indexing annotation must be entered when the overall report is classified)

1 ORIGINATING ACTIVITY (Corporate author)

Spectran, Inc
941 Highland Ave
Hollywood, CA 90028

2a. REPORT SECURITY CLASSIFICATION: Unclassified

2b. GROUP:

3 REPORT TITLE

DIAL PACK DUST CLOUD DATA ANALYSIS

4 DESCRIPTIVE NOTES (Type of report and inclusive dates)

Final Report

5 AUTHOR(S) (First name, middle initial, last name)

J. C. Auckland

6 REPORT DATE	7a. TOTAL NO. OF PAGES	7b. NO. OF REFS
1 Mar 1972	64	

8a. CONTRACT OR GRANT NO: F30602-71-C-0297

b. [redacted]

Army MIPR Number: A31699-13-Z575

c.

d.

9a. ORIGINATOR'S REPORT NUMBER(S)

9b. OTHER REPORT NO(S) (Any other numbers that may be assigned this report)

RADC-TR-72-68

10 DISTRIBUTION STATEMENT

Approved for public release; distribution unlimited.

11 SUPPLEMENTARY NOTES

Monitored by
Rome Air Development Center (OCS)
Griffiss AFB, NY 13440

12. SPONSORING MILITARY ACTIVITY

U.S. Army Ballistic Missile Defense Agency
1320 Wilson Blvd
Arlington, VA 22209

13 ABSTRACT

Properties of the atmosphere can be measured directly or indirectly. Direct measurements provide point measurement accuracies but indirect or remote sensing techniques permit probes of a large volume at times when direct measurements may not be possible. Event Dial Pack in July of 1970 is an example of such a condition. This report discusses measurements made by 10.2 and 30 GHz microwave radiometers upon the dust clouds during that experiment and the results of a detailed analysis upon that data.

DD FORM 1 NOV 65 1473

UNCLASSIFIED

Security Classification

14 KEY WORDS	LINK A		LINK B		LINK C	
	ROLE	WT	ROLE	WT	ROLE	WT
Propogation Radiometric Analysis						

DIAL PACK DUST CLOUD DATA ANALYSIS

J. C. Auckland

Spectran Incorporated

Approved for public release;
distribution unlimited.

This research was supported by the
U.S. Army Advanced Ballistic Missile
Defense Agency and was monitored by
RADC (OCS), GAFB, NY 13440 under
Contract No. F30602-71-C-0297.

FOREWORD

The following report presents the results of a study program for the analysis of the microwave radiometric data collected during Event Dial Pack in July of 1970. Additional microwave radiometric data was collected at 10.2 GHz and 30 GHz to support the analysis.

The assistance of RADC is acknowledged in obtaining samples of Canadian soil in the test area. Special recognition should be given to the National Environmental Technology Laboratories, Inc., for their assistance in analysis of the microwave radiometer and radar data.

PUBLICATION REVIEW

This technical report has been reviewed and is approved.

RADC Project Engineer

TABLE OF CONTENTS

ILLUSTRATIONS

TABLES

SECTION 1

INTRODUCTION

The properties of an atmosphere can be investigated by direct methods and indirect methods. The direct methods have the advantage of providing accurate point measurements, but the sampling of large volumes is difficult or impossible. The **indirect** methods, passive and active, permit probing of very large volumes with loss of point accuracy. There are, of course, cases where only one or neither of the methods can be usefully employed.

The Event Dial Pack of 23 July 1970 provides a specific example of a situation where indirect methods of probing can be gainfully employed. During the early phases of such an event, it is extremely difficult to obtain in situ measurements while both radar and microwave radiometer techniques yield useful data, though they require careful interpretation. This report presents the results of a program directed toward analyzing the microwave radiometric data obtained during Event Dial Pack.

Additional microwave radiometric data was taken during this program in a controlled environment to support the analysis. Both active and passive data were analyzed as this event represents the only known experiment of its type when both techniques can be compared.

TECHNICAL BACKGROUND

1. GENERAL

The microwave emission of the clear atmosphere viewed by a radiometer from the ground is unpolarized. When the atmosphere becomes turbid due to the presence of suspended material, observed radiation intensities increase and possibly also exhibit a degree of polarization. The cause of the polarization is the presence, in sufficient numbers, of particles with high scattering efficiencies, and observed polarization can be the result of the scattering process and/or a property of the radiation impinging on these particles. It is possible from spectral measurements of cross polarized intensity to determine the properties of the suspended matter when illuminating intensities are specified.

2. THE MEASUREMENTS

The measurements performed during Event Dial Pack consist of the time histories of the horizontal and vertical polarized components of the dust cloud's radiation field at 10.2 and 30 GHz. During the detonation and cloud rise phase of the observations,

the radiometers were directed such that the line-of-sight passed directly over ground zero. Following detonation, the dust cloud ascended through the radiometer field of view. During the second phase the elevation angle was increased to 48.5 degrees to observe the overhead passage of the cloud. A boresighted camera provided pointing information for interpretive purposes.

3. THE PROBLEM

The specific problem considered during the experiment was the determination of physical properties of a near-earth dust cloud from microwave radiometric observation. Unfolding the total time-dependent radiation field to yield the properties of the cloud was complicated by the temporal microphysical and macrophysical properties of the cloud, pertinent geometry, and the characteristics of the radiometers. In addition, the spatial distribution of natural sources of radiation, i.e., the ground, atmosphere, and sun, played a role in the thermalization of the cloud as well as being contributing sources if scattering is an important mechanism. Short of developing a complete and general solution to this involved problem, approximations and idealizations can be employed in models of the physical situation to isolate important mechanisms, provide an explanation for observed intensities and polarizations, and to recover certain properties of the cloud. A goal of eventually obtaining the full formal solution was in mind during the program.

4. STATEMENT OF WORK

The proposed tasks for this program fall into three major categories - namely microwave data analysis, scattering phenomena analysis, and passive-active signal comparisons. Specific tasks to be performed are outlined as follows:

a. Microwave data analysis

(1) Reduce radiometer voltages to equivalent transmission losses.

(2) Estimate beamfill ratio of the cloud versus time.

(3) Calculate the normalized insertion loss from cloud dimensions and positions as a function of time.

(4) Conduct a set of simple tests to measure small particles with a microwave radiometer to determine their signature under laboratory conditions.

(5) Measure the dielectric constant of actual test samples.

b. Scattering Phenomena

(1) Determine the primary mechanisms responsible for the observed dust cloud microwave brightness temperatures and polarizations.

(2) Formulate the mathematical model relating the observed brightness temperatures to the test geometry in terms of the primary radiation transfer mechanism.

(3) Analyze the existing radiometric measurements in accordance with the mathematical model to determine the dust cloud parameters.

(4) Recommend procedures for optimizing data return from microwave radiometric measurements in future experiments.

c. Passive-Active Signal Comparisons

(1) Compare radar (X and K_a band) returns with radiometric signals.

(2) Calculate back scattering signals to be expected from cloud models obtained above. Iterate model and measured returns to refine microwave models.

(3) Calculate complete scattering from dust cloud.

The discussions which follow do not necessarily follow the outlined format in the Statement of Work as the tasks are category groupings only. The microwave experimental data collected during the program was specifically oriented toward supporting the analysis of Event Dial Pack data.

No major difficulties were encountered in performing all tasks except for differentiating cloud thermal changes from insertion loss changes. The radar data was very minimal for a full comparative analysis.

5. MEASUREMENTS

a. General

The measurements reported upon herein were conducted to provide ancillary data to that obtained during Event Dial Pack. All experiments were conducted under controlled conditions for the purpose of determining attenuation, polarization and refractive properties on dust particles. These measurements were necessary to assure that the analysis was approached in a meaningful way.

The data was further reduced during the program to provide beamfill data for the microwave radiometer antennas. These data along with dielectric constant data are required for an evaluation of insertion loss and transmission loss.

b. Experimental Data

(1) Transmission Loss Data

Initially the experiments of this program were planned as scaled simulations of Event Dial Pack dust clouds. The clouds were to be created at close range with a constant density and dust particle size. Subsequent post contract evaluation indicated that the proposed approach was too difficult to instrument with any accuracy and that cloud density could not be controlled for 100% antenna beamfill.

An alternate solution was used which proved to be satisfactory, in which density could be simulated and easily controlled. Instead of creating dust clouds, sheets of dry foam were placed directly in front of the antennas with the antennas aimed at the zenith. Sand was weighed, measured and evenly spread over the foam in the antennas' field of view.

Some uncertainties exist with this technique, in that the dust particles are now in the near field of the antenna. Experiments with larger targets show that the effects, if any, on the data are small as the signals measured are noncoherent noise. Uncontrolled differencies in the simulation are sidelobe and backlobe contributions.

Curves of differential temperature versus ounces of sand are shown in Figures 1 and 2. These data represent both vertical and horizontal polarized signals as no differences were noted after corrections were made for gain differences. The sinusoidal nature of the curves should be noted. This characteristic is typical of abrupt interfaces between materials of differing dielectric constants. Each complete cycle represents one-half wavelength of material thickness. Damping of the sinusoid represents the losses in the material. For large dust clouds, this effect should disappear.

(2) Dielectric Measurements

The dielectric constants of the materials used during this program were measured using a large coaxial line

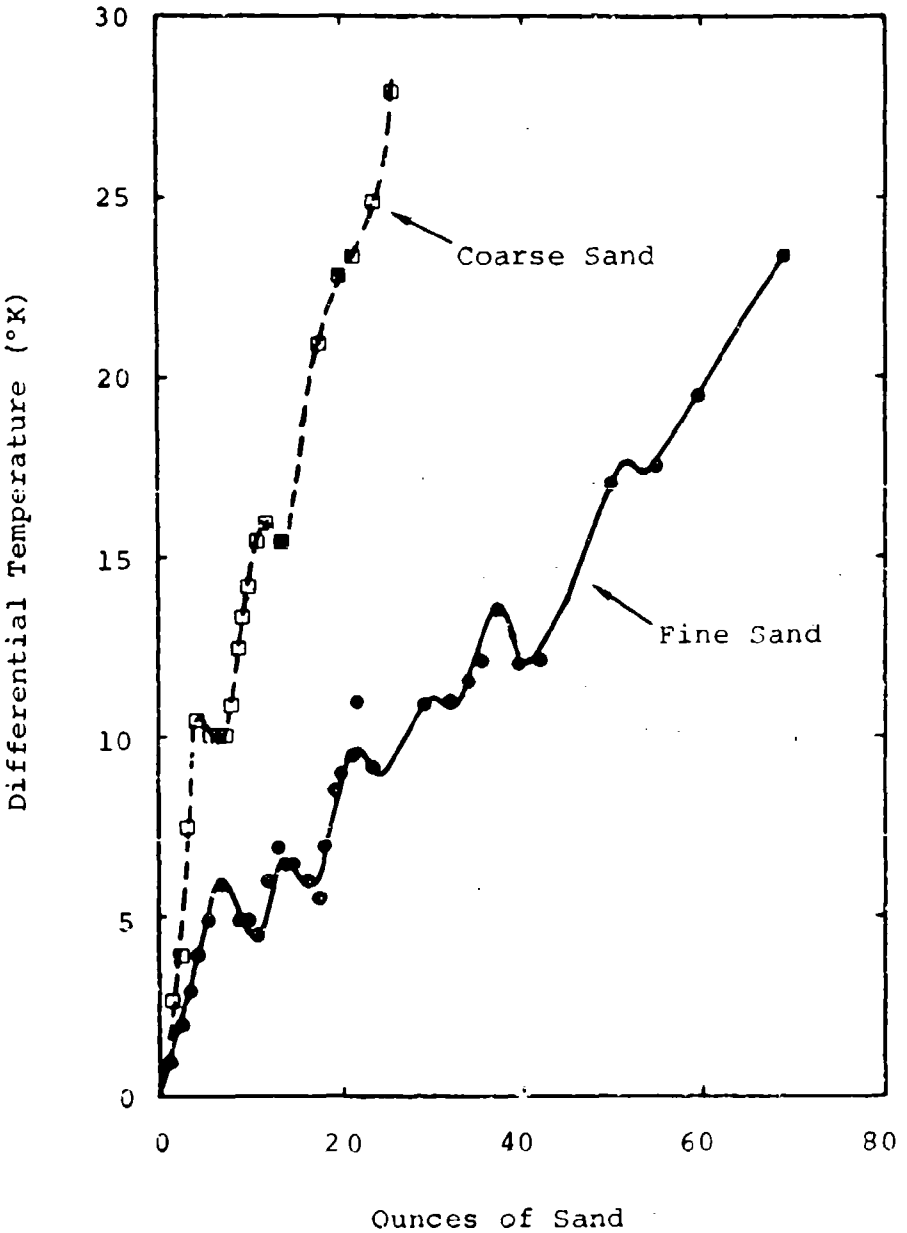

Figure 1 - 30 GHz Differential Radiometric Temperature

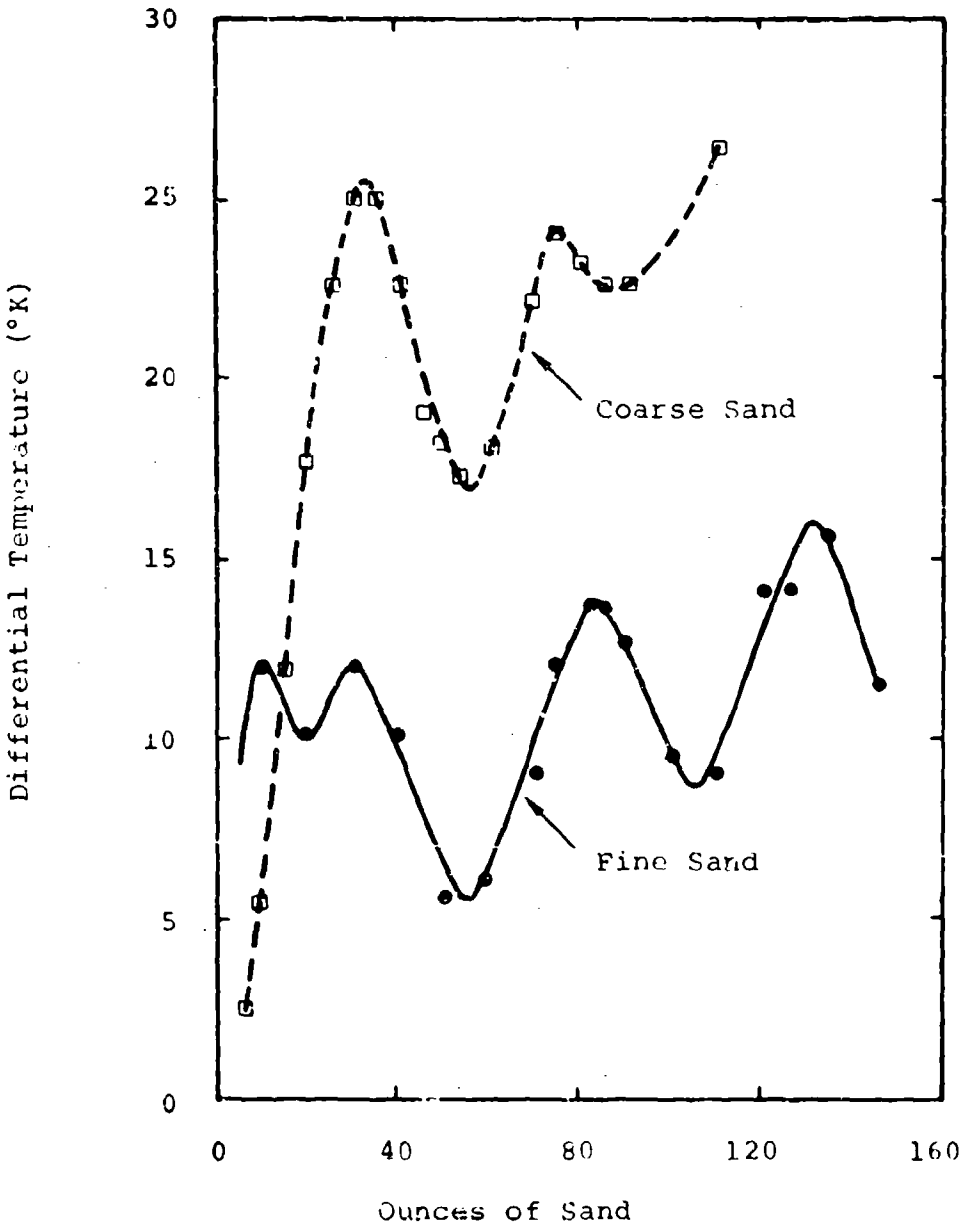

Figure 2 - 10.2 GHz Differential Radiometric Temperature

terminated in 50 ohms. Materials were placed in the dielectric region of the coaxial line and reflection coefficients were measured using a Time Domain Reflectometer (TDR) technique. The dielectric constants for the fine and coarse sands used were 2.64 and 3.51, respectively. Samples of fine and coarse Canadian soil were obtained after the measurements portion of this program; however, dielectric measurements were made in the same manner and found to be 3.86 and 4.40 for the fine and coarse soil, respectively.

(3) Antenna Beamfill Ratio

The only means for evaluating antenna beamfill ratio during Event Dial Pack was from the 16mm movie boresight camera film. The camera had a 25mm lens and microwave radiometer antenna half-power (3db) beamwidths were 4.0 degrees at 10.2 GHz and 2.4 degrees at 30 GHz. Thus, the antenna beam's intercept area could be calculated assuming the dust cloud distance to be equal to ground zero. An overlay was constructed equal to this area and percentage beamfill was measured from the film. A plot of beamfill ratio calculated by this technique is shown in Figure 3. Beamfill ratios after panning to the cloud were always 100%.

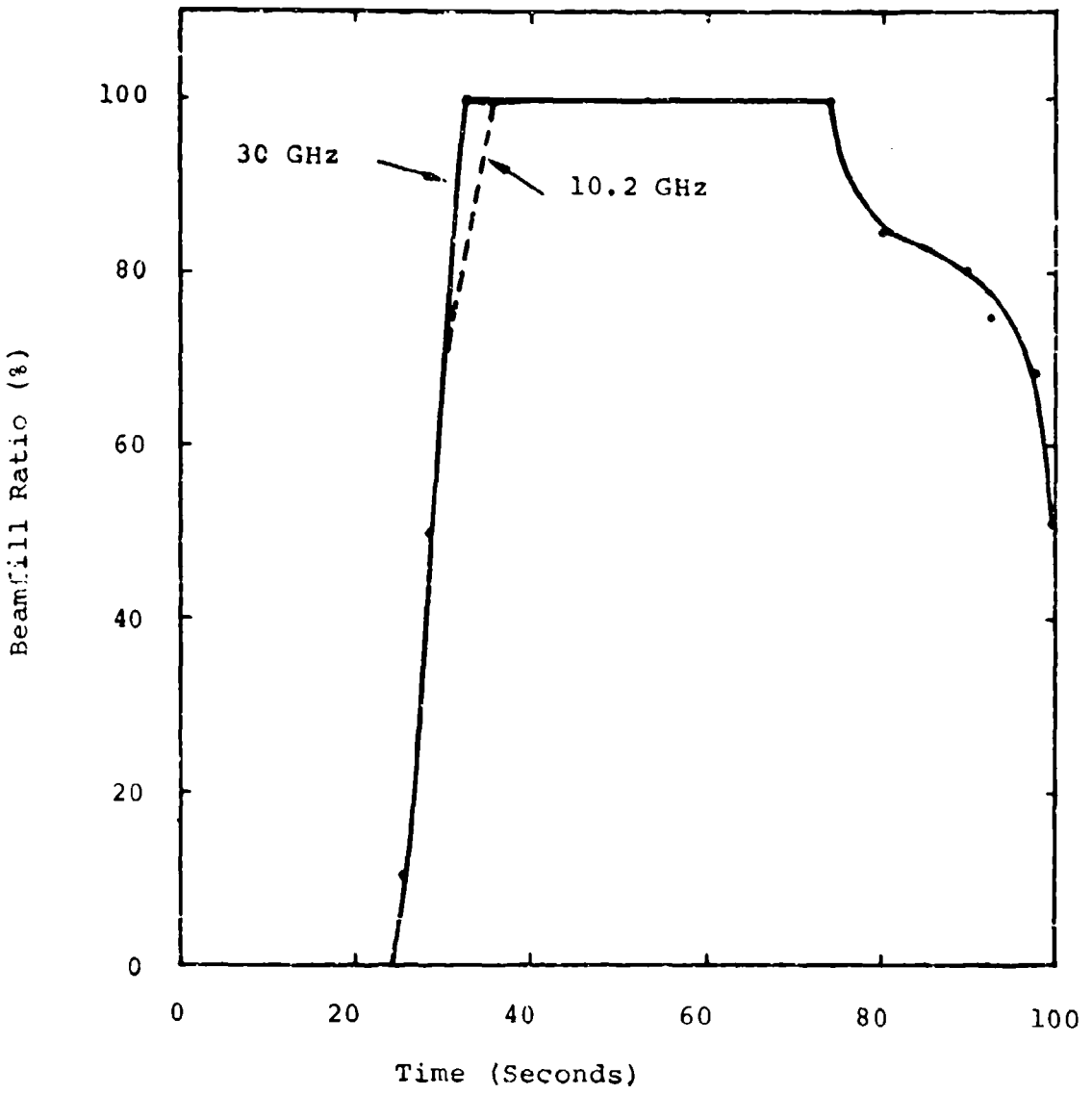

Figure 3 - Antenna Beamfill Ratio (Cloud Stem Only)

SECTION II

ANALYSIS

1. GENERAL

The approach taken during the analysis was to first examine the radiative properties of dust particle distributions obtained by aircraft sampling at times exceeding 10 minutes after detonation. As earlier aircraft data was not available, a variety of extrapolations to earlier times were made in an attempt to simulate early phase radiometric observations.

A second approach, whereby particle refractive index and an arbitrary particle size distribution would have been subjected to iterative adjustment to match emission, polarization and radar backscattering observations, was abandoned for lack of reliable data. This second approach would have provided an assessment of the validity of the extrapolation of physical sampling data along with an alternate determination of cloud radiation properties.

2. QUALITATIVE DATA INTERPRETATION

The data acquired during the Event Dial Pack is shown in Figure 4. Time progresses to the left and all significant events are labeled. The outputs of the horizontally and vertically polarized receiver channels, designated H and V, respectively, are displayed for both 10.2 GHz and 30 GHz. The differences, H-V, which are proportional to polarization are also displayed. Calibrations for all channels are 1°C per millivolt, giving 25°C full scale for the H and V channels and 5°C full scale for the polarization difference channels.

The results for 10.2 GHz radiometer are shown in the top three traces. These data are contaminated by signals from a nearby radar, which prior to the event were directed away from ground zero and toward the radiometer location. At T_o, this radar was pointed toward ground zero, but some interference is still evident. As the level of this interference does not appear to be time dependent, it is concluded thatradar energy scattered from the cloud toward the radiometers is not detectable.

The behavior of the polarization channel, although irregular and indicating some degree of polarization, was difficult to interpret. Figure 5 gives boresight camera frames corresponding to the times labeled 1-4 on the strip chart record. Thus, at time 2, the radiometers were boresighted on the cloud, and as the geometry of Figure 6 depicts, the radiometer beams were completely filled. The H and V channels follow each other quite closely from the beginning of the cloud rise through time 4. A notable characteristic of these records is that the polarization channel exhibited

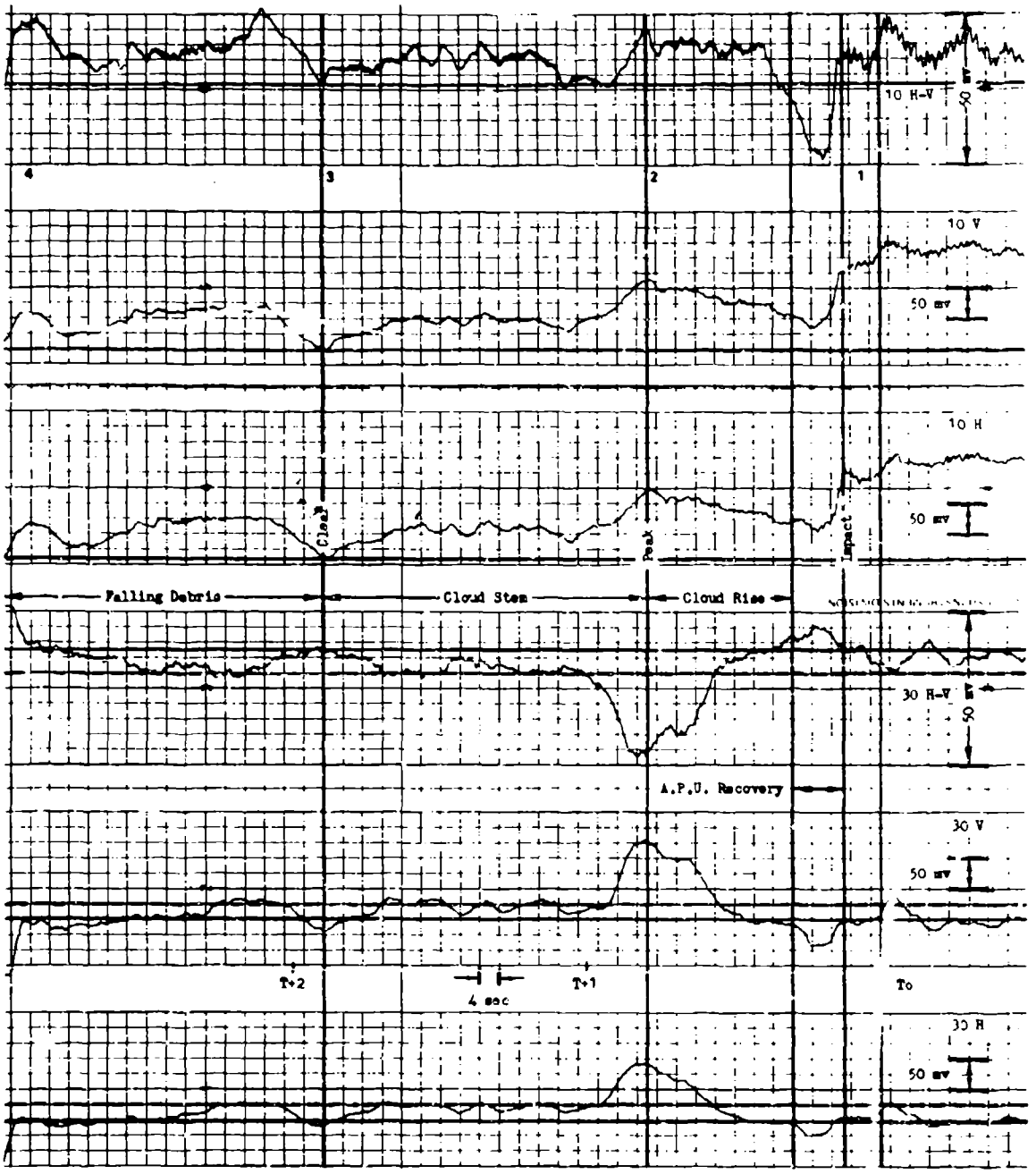

Figure 4 - 10 GHz and 30 GHz Radiometric Response
(View Angle = 17° above the horizon)

DASA 2589

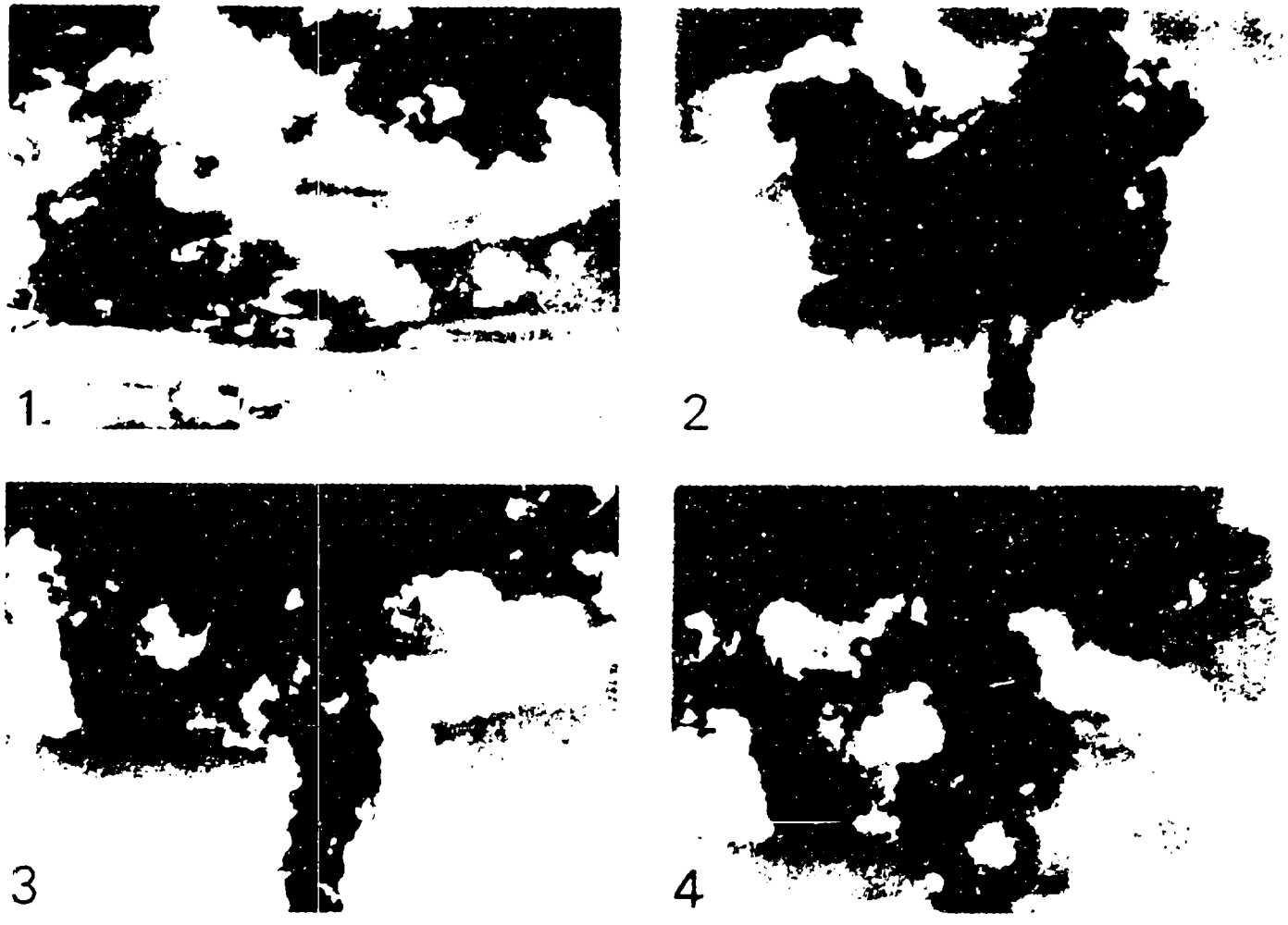

Reproduced from best available copy

Figure 5 - 16 mm Photographs of the Event Dial Pack
(Numbers refer to similar numbers on Figure 4)

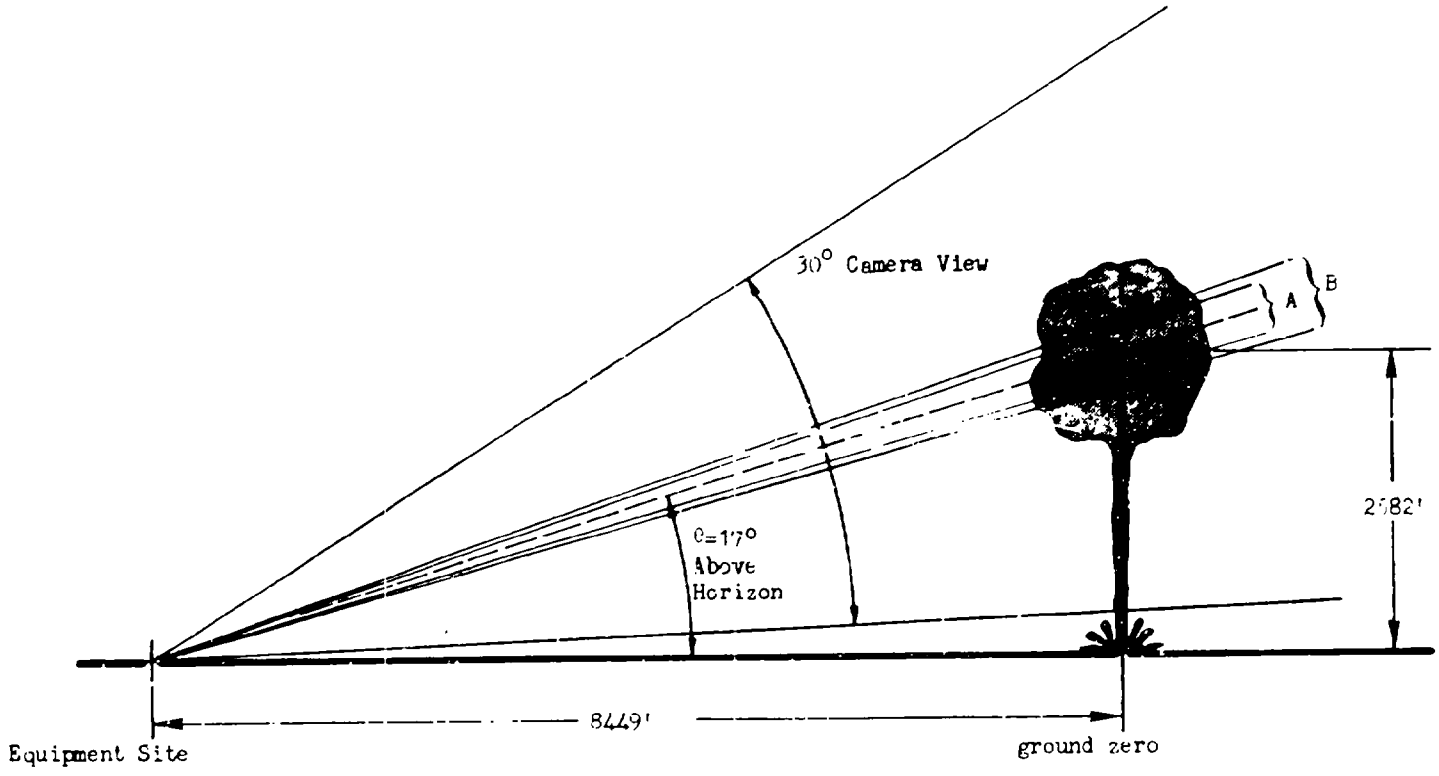

Camera Height View = 5000' @ 8449'
(A) 2.4° Antenna = 390' dia. @ 8449'
(B) 4.0° Antenna = 640' dia. @ 8449'

Scale: $\frac{1}{4}$" = 338'

Figure 6 - Diagram of Experiment Geometry

its largest excursions when the rate of change of H and V were greatest. The conclusion is that small differences in gain, time constant, H and V plane beam shapes, and nonlinearity are the most probable causes of the apparent small and variable degree of polarization.

The results from the 30 GHz radiometer are shown in the bottom three traces of Figure 4. If the radiation received from the direction of the cloud truly possess a degree of polarization, it should be evident in this data.

The immediate striking feature of the 30 GHz records is the large change in the polarization occurring when the rising cloud passes through the radiometer field of view. Otherwise, the polarization channel exhibits little variability and substantiates the conclusion arrived at from examination of the 10.2 GHz data.

Closer scrutiny of the H and V traces shows that while they follow each other closely, the peak-to-peak excursions of the larger scale structure shows evidence of differential gain. As there appears to be no radar interference, the ratio of the peak-to-peak excursions on the two channels can be scaled for the short period just prior to T_o. During this period, clear sky and broken cumulus clouds were in the field of view so that polarization would not be expected. The ratio $\Delta H/\Delta V$ is approximately 0.67. The ratio of the changes in H and V due to the dust cloud at time 2 is also approximately 0.67. From this, it was concluded that differential gain existed and that the vertical channel had the highest gain. If the polarization channel is corrected for the indicated amount of differential gain, the amplitude of its variations over the entire record is reduced to noise.

The true degree of polarization, π, would be less than or equal to (H-V)/(H+V). Therefore, if the absolute base radiation levels were assumed to be zero, and if differential gain were ignored, the degree of polarization at time 2 would be

$$\pi \leq \frac{45}{90+135} = 0.20$$

or approximately 20 percent. To be more realistic, however, a background level of 40°K, which corresponds to a base level of 400 mv, can be assumed (see Figure 7). Under this assumption

$$\pi \leq \frac{45}{490+535} = 0.0439$$

or approximately 4.4 percent. This would be a measurable and significant amount of polarization. However, when differential gain is accounted for, the degree of polarization becomes inconsequential.

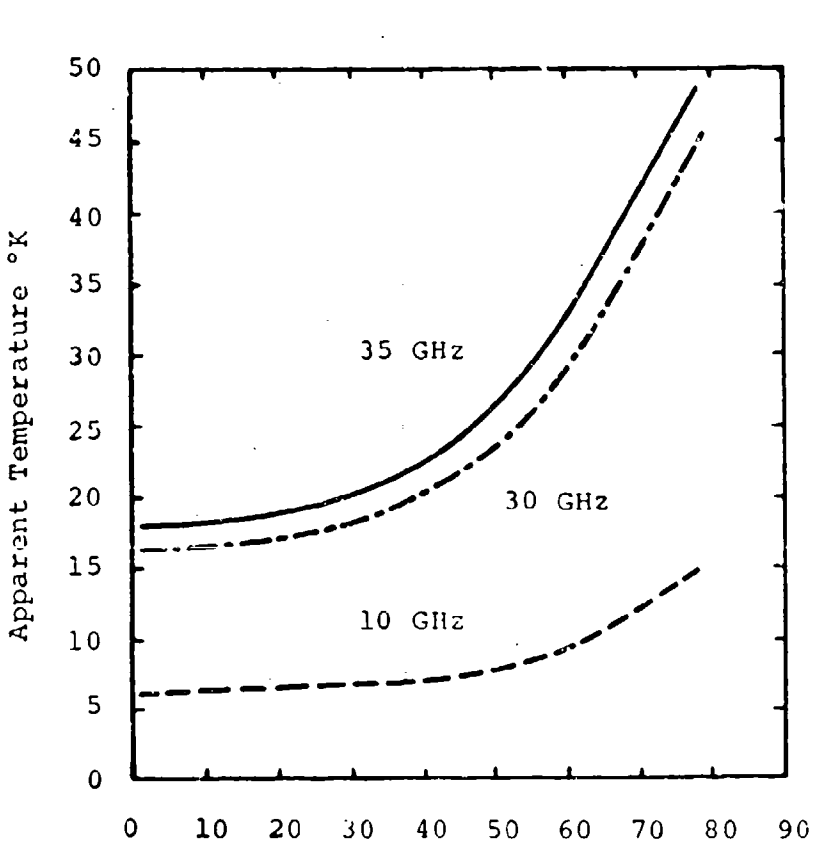

Figure 7 - Sky Brightness Temperatures for
A Clear Standard Atmosphere

Despite the conclusions of this qualitative look at the data, the problem was further examined, using all available data, first with Rayleigh calculations and then with extensions to Mie theory. After this, a final assessment of the microwave radiometric data and its significance was made.

3. RAYLEIGH APPROXIMATIONS - LATE PHASE

As a starting point to quantitative analysis, the aircraft particle sampling data for Event Dial Pack, pass #1,* T_o + 11 minutes, are examined and then used as the basis for calculations. The particle size distribution is given in Table I. For this distribution of 669 particles, the average particle size (diameter) is 59 microns, giving a circumference to wavelength ratio ($x = \pi d/\lambda$) of 0.018 at 30 GHz, well within the Rayleigh criteria. Even the largest particles in the distribution (300μ) have the size parameter $x < 0.1$. It is therefore assumed that the Rayleigh approximations for extinction and absorption are valid.

a. The Equivalent Volume Radius

If all of the particles in a size distribution are within the Rayleigh range, then the true distribution can be replaced for computational purposes by the same total number of particles of equivalent volume radius, r_e. By this procedure, the extinction cross-section, σ_{ex}, and the volume extinction coefficient, β_{ex}, can be simply calculated by algebraic means.

The volume, V_D, of the 669 dust particle is given by the summation

$$V_D = \frac{4\pi}{3} \sum_{i=1}^{24} D(r_i) r_i^3 \qquad (1)$$

where $D(r_i)$ is the tabulated dust particle size distribution of Table I and r_i is particle radius. The subscript i has been introduced to indicate the discrete sample values. Performing this numerical integration produces the following table of values (Table II) with the result that $V_D = 3.75 \times 10^8\ \mu^3$. Equating V_D to the volume of 669 particles of radius r_e and then solving for r_e gives

$$r_e = 51\mu$$

---

*Report DASA 2600, MR170, FR-948

TABLE I

DUST PARTICLE SIZE DISTRIBUTION FOR PASS #1*

Diameter μ	Number of Particles	Diameter μ	Number of Particles
10	4	130	17
20	9	140	9
30	65	150	14
40	86	160	10
50	95	170	9
60	85	180	4
70	68	190	7
80	49	200	9
90	39	220	1
100	37	250	5
110	25	300	1
120	20	350	1

Mean Particle Diameter - 59μ

Total Number of Particles - 669

Total Dust Collected - 13.9 ± 1.0mg

Sampling Times: On T_o + 10 minutes, 51 seconds
Off T_o + 11 minutes, 32 seconds

Total Volume Sampled - 1.82m^3

Cloud Width - 1920m

* Data taken from Report DASA 2600 MR170 FR-948

TABLE II

Table of Values for Calculating the Equivalent Volume of the Pass #1 Particle Distribution

i	$D(r_i)$	$r_i(\mu)$	$r_i^3(\mu^3)$	$\Delta V_D(\mu^3)$
1	4	5	1.25×10^2	2.09×10^3
2	9	10	1.00×10^3	3.77×10^4
3	65	15	3.38×10^3	9.17×10^5
4	86	20	8.00×10^3	2.88×10^6
5	95	25	1.56×10^4	6.21×10^6
6	85	30	2.70×10^4	9.61×10^6
7	68	35	4.29×10^4	1.22×10^7
8	49	40	6.40×10^4	1.31×10^7
9	39	45	9.11×10^4	1.49×10^7
10	37	50	1.25×10^5	1.94×10^7
11	25	55	1.66×10^5	1.74×10^7
12	20	60	2.16×10^5	1.81×10^7
13	17	65	2.75×10^5	1.96×10^7
14	9	70	3.43×10^5	1.29×10^7
15	14	75	4.22×10^5	2.48×10^7
16	10	80	5.12×10^5	2.14×10^7
17	9	85	6.14×10^5	2.31×10^7
18	4	90	7.29×10^5	1.22×10^7
19	7	95	8.57×10^5	2.51×10^7
20	9	100	1.00×10^6	3.77×10^7
21	1	110	1.33×10^6	5.57×10^6
22	5	125	1.95×10^6	4.08×10^7
23	1	150	3.38×10^6	1.42×10^7
24	1	175	5.36×10^6	2.24×10^7

$$V_D = 3.745 \times 10^8 \ \mu^3$$

This equivalent particle radius is 1.73 times larger than the average particle radius of 29.5μ for the distribution and the corresponding value of wavelength ratio x at 30 GHz is 0.032, well within the Rayleigh criteria. Note that no significance should be given to r_e other than its value in simplifying calculations.

b. Simulation Experiment Results

Changes in measured apparent temperature were recorded as a function of the total weight in ounces of the sand, which was spread uniformly over a polyurethane sheet (Figures 1 and 2). This data as a function of mass per unit column for the 30 GHz radiometer vertical polarization channel for both grades of sand is shown in Figure 8. The periodicities can again be noted by inspection of individual points. Analyses of the data show that 9.8 ounces of coarse sand and 38 ounces of fine sand were required to cause an increase of 13.5°C in apparent temperature, as observed during Event Dial Pack. These weights of sand correspond to layer thickness of 0.225 cm and 1.059 cm, respectively. The mass in a centimeter square column was 0.387 gms for coarse sand and 1.52 gms for fine sand. Results for horizontal polarization are not given, as they were consistent with those of the vertical channel, as was expected.

The values cited above may not be exact as the layers of sand were in the near field, but are sufficient for the comparisons to be made. It is expected that sand particles in suspension may not yield the same results and that considerably more mass per unit column would be required for comparable extinction properties. The excess required mass depends on the particle dielectric properties and size distribution.

At 10.2 GHz the experimental data was more difficult to interpret because of sinusoidal interference effects, but it appears that approximately 10 ounces of each grade of sand gives rise to the 5.5°C increase in apparent temperature as observed during Event Dial Pack.

The modulus of the dielectric constant, ε_1, for the coarse sand was determined to be 3.51, while that of the fine sand was 2.64. As the loss tangent can only be implied by the slope of the curve, computer model calculations for dust with the refractive properties of these coarse and fine sands were made for imaginary parts of the refractive index of 0.01, 0.005 and 0.001. Hand calculations were made using approximate formulas for 0.005, i.e., $m = (\varepsilon_1) - i0.005$.

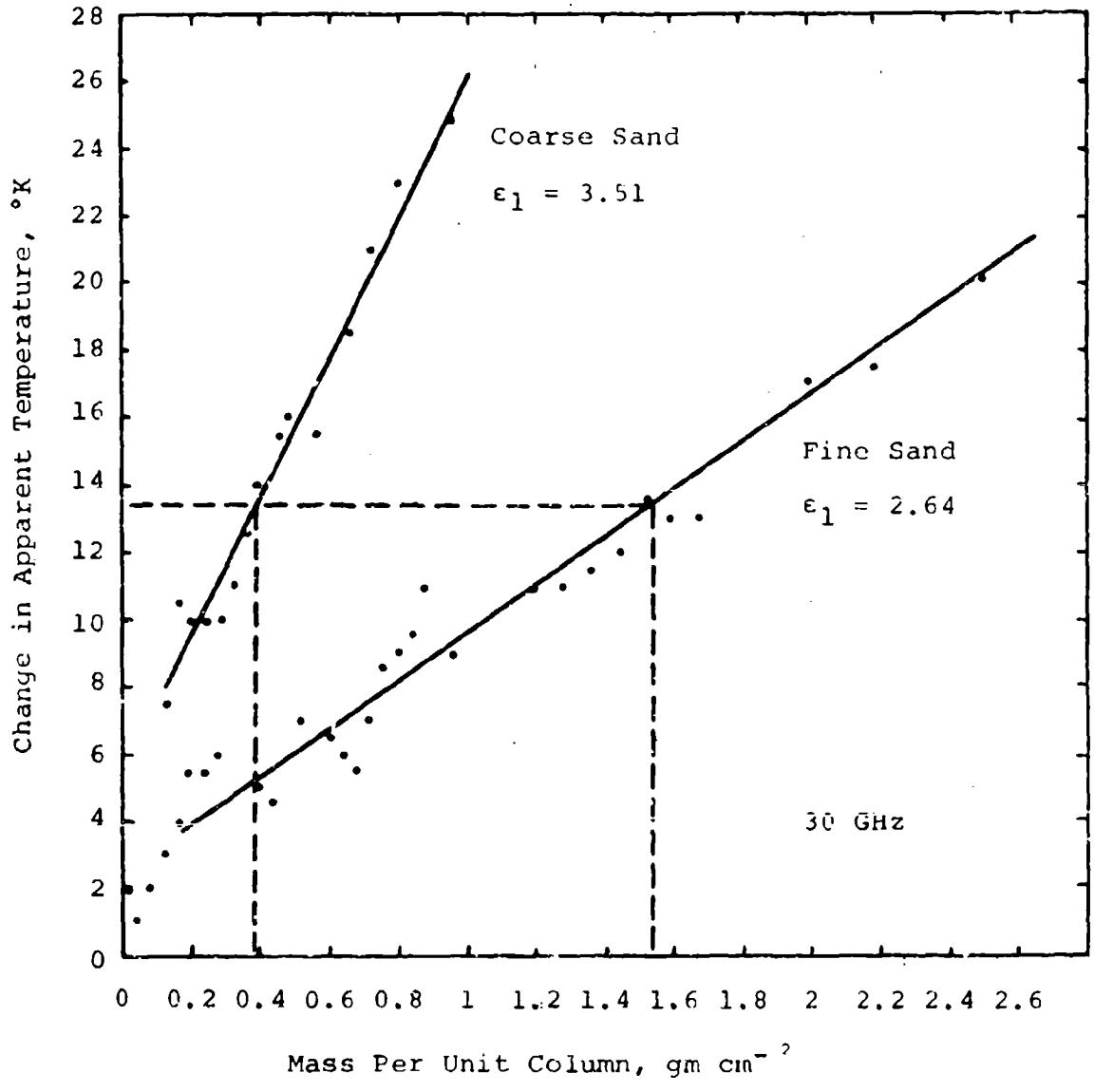

Figure 8 - Change in Apparent Temperature Versus Columnar Content of Sand

c. The Volume Extinction Coefficient

Using the equivalent volume radius, r_e, for the dust particle distribution of pass #1, the volume extinction coefficient for the dust cloud at T + 11 minutes can be calculated. First, the particle extinction cross section, σ_{ex}, is calculated from[1]

$$\sigma_{ex} = 48\pi^2 r_e^3 \frac{\nu\kappa}{Z_1\lambda} \qquad (2)$$

where

ν = real part of dust particle refractive index
κ = imaginary part of dust particle refractive index
λ = wavelength of radiation

and

$$Z_1 = (\nu^2+\kappa^2)^2 + 4\ (\nu^2-\kappa^2) + 4$$

Then, substituting $r^3 = 1.34\times10^{-7}$ cm^3, the particle extinction cross-sections for λ = 1cm and λ = 2.94cm, respectively, (designated by superscripts k, x) are found to be

	m = 1.88-i0.005	m = 1.63-i0.005
σ_{ex}^k (cm^2) =	1.	2.37×10^{-8}
σ_{ex}^x (cm^2) =	6.6	8.06×10^{-9}

The volume extinction coefficients, β_{ex}, can now be calculated using particle densities. From pass #1 data, there were 669 particles collected from 1.82m^3 of cloud. Therefore, a particle density of 3.68×10^{-4} per cm^3 is arrived at and the corresponding extinction coefficients are

	m = 1.88-i0.005	m = 1.63-i0.005
β_{ex}^k (cm^{-1}) =	7.13×10^{-12}	8.72×10^{-12}
β_{ex}^x (cm^{-1}) =	2.43×10^{-12}	2.97×10^{-12}

[1]Penndorf, R. B., "Scattering and Extinction Coefficients for Small Absorbing and Non-Absorbing Aerosols," J. Opt. Soc. Amer., Vol. 52, No. 8, August 1962, pp. 896-904.

d. Optical Thickness and Transmittance

The optical thickness of the cloud, τ, is defined by

$$\tau = \int_0^W \beta_{ex}(s)\, ds \qquad (3)$$

and if it is assumed that β_{ex} is independent of position, s, then

$$\tau = \beta_{ex} W \qquad (4)$$

where W is the width of the cloud. Working under this assumption (particle distributions as a function of position are not available), the optical thickness for the respective wavelengths, using the cloud width of 1.92 km for pass #1 are

	m = 1.88-i0.005	m = 1.63-i0.005
τ^k =	1.37×10^{-6}	1.67×10^{-6}
τ^x =	4.67×10^{-7}	5.70×10^{-7}

Transmittance is related to optical thickness by

$$t = \exp(-\tau) \qquad (5)$$

from which we obtain

	m = 1.88-i0.005	m = 1.63-i0.005
t^k =	1-0.00000137	1-0.00000167
t^x =	1-0.000000466	1-0.000000570

These results indicate that at T = 11 minutes, the cloud is for all practical purposes transparent at wavelengths of 1 and 2.94 cm. Reference to Figure 9 establishes this to be the case, as the radiometers are obviously seeing background radiation. There was no need to consider the relative importance of scattering and absorption in this case, but since a comparison of scattering coefficients is made at a later point, the volume scattering coefficient β_{sc} is next calculated.

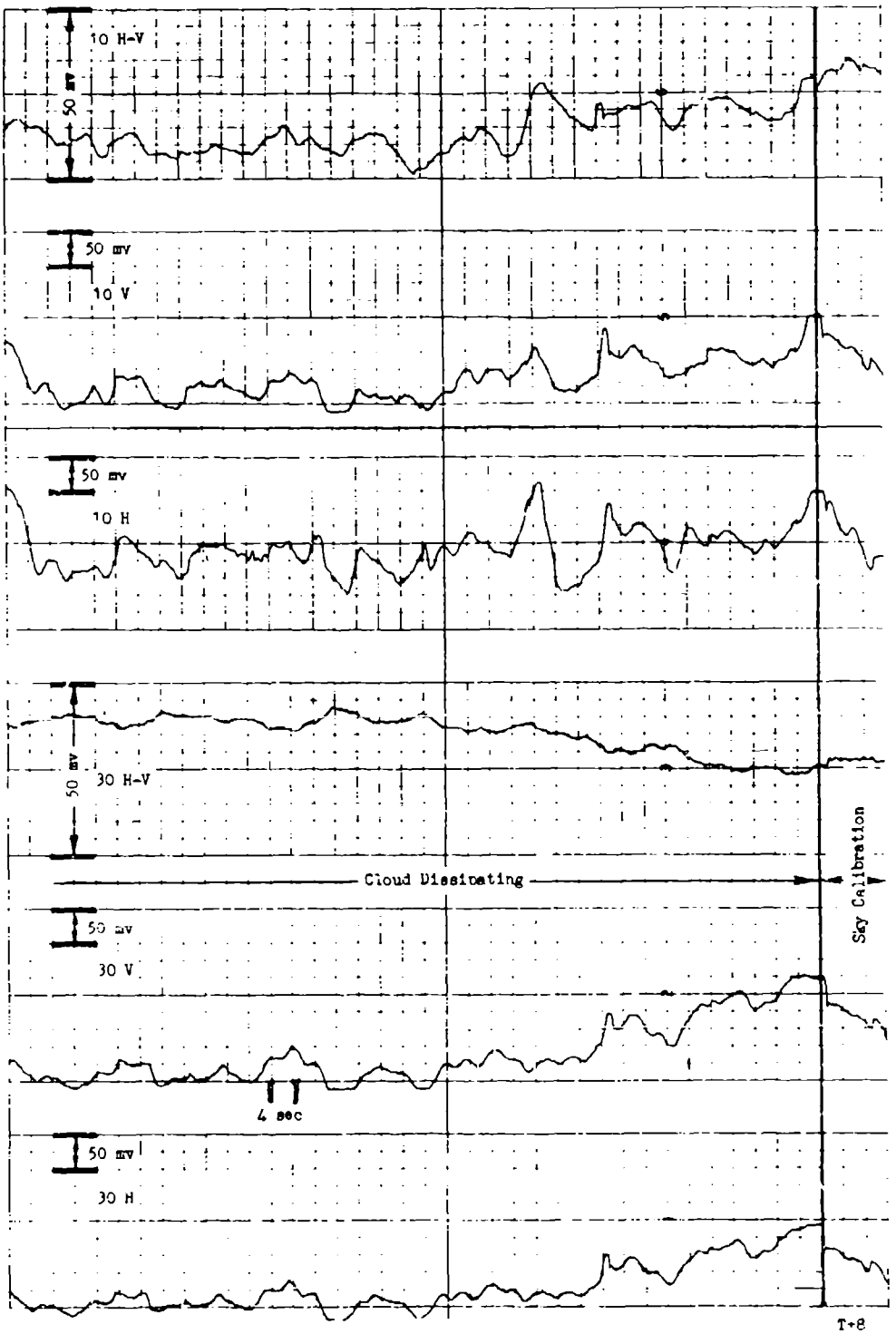

Figure 9 - 10 GHz and 30 GHz Radiometric Response
(View Angle = 48.5° above horizon)

DASA 2589

e. The Equivalent Volume-Squared Radius

Previously, the equivalent volume radius was determined for use in calculating the extinction coefficients. However, when using r_e in the Rayleigh formula for scattering cross section, a significant underestimate results. Experience has shown that an alternate radius, the equivalent volume-squared radius r_{vv}, defined by

$$r_{vv}^3 = \left\{ \frac{\sum_{i=1}^{24} D(r_i)\, r_i^6}{\sum_{i=1}^{24} D(r_i)} \right\}^{1/2} \qquad (6)$$

produces accurate values for the scattering coefficients.

With the aid of the following table of values (Table III), the volume-squared for the pass #1 particle size distribution, V_{D2}^2, is found to be $1.88 \times 10^{15}\ \mu^6$. Normalizing V_{D2}^2 to the total number of particles and solving for r_{vv} gives

$$r_{vv} \cong 74\mu$$

This equivalent particle radius is 2.5 times larger than the average particle radius and 1.45 times larger than r_e, but is also well within the Rayleigh range with the corresponding value of x of 0.046. As with r_e, r_{vv} should be given no special significance.

f. The Volume Scattering Coefficient

Under the assumptions that the cloud is optically thin ($\tau << 1$) and that single scattering governed by Rayleigh laws holds, extinction, absorption and scattering are related by

$$\beta_{ex} = \beta_{ab} + \beta_{sc} \qquad (7)$$

The alternative therefore exists for calculating β_{sc} directly or indirectly through the calculation of β_{ab}. The first alternative was chosen here because of its simplicity. The particle scattering cross-section, β_{sc}, can be calculated using

TABLE III

Table of Values for Calculating the Equivalent Volume-Squared of the Pass #1 Particle Distribution

i	$D(r_i)$	$V_{D2}(\mu^3)$	$D(r_i)\Delta V_{D2}(\mu^6)$
1	4	5.23×10^{2}	1.10×10^{6}
2	9	4.19×10^{3}	1.58×10^{8}
3	65	1.42×10^{4}	1.31×10^{10}
4	86	3.35×10^{4}	9.63×10^{10}
5	95	6.54×10^{4}	4.07×10^{11}
6	85	1.13×10^{5}	1.09×10^{12}
7	68	1.80×10^{5}	2.20×10^{12}
8	49	2.68×10^{5}	3.52×10^{12}
9	39	3.82×10^{5}	5.69×10^{12}
10	37	5.24×10^{5}	1.02×10^{13}
11	25	6.96×10^{5}	1.21×10^{13}
12	20	9.05×10^{5}	1.64×10^{13}
13	17	1.15×10^{6}	2.24×10^{13}
14	9	1.44×10^{6}	1.86×10^{13}
15	14	1.77×10^{6}	4.38×10^{13}
16	10	2.15×10^{6}	4.62×10^{13}
17	9	2.57×10^{6}	5.94×10^{13}
18	4	3.06×10^{6}	3.74×10^{13}
19	7	3.59×10^{6}	9.03×10^{13}
20	9	4.19×10^{6}	1.58×10^{14}
21	1	5.57×10^{6}	3.10×10^{14}
22	5	8.17×10^{6}	3.34×10^{14}
23	1	1.42×10^{7}	2.02×10^{14}
24	1	2.25×10^{7}	5.06×10^{14}

$V_{D2}^2 = 18.80\times10^{14}\ \mu^3$

(from Deirmendjian[2])

$$\sigma_{sc} = 24\pi^3 \left|\frac{m^2-1}{m^2+2}\right|^2 \frac{\left[\frac{4\pi}{3} r_{vv}^3\right]^2}{\lambda^4} \qquad (8)$$

where $m = \nu - i\kappa$ = particle complex index of refraction.

Note that the equivalent volume-squared radius just derived is used in this expression. The resulting scattering cross-sections and volume scattering coefficients for the two measurement wavelengths are

	$m = 1.68-i0.005$	$m = 1.63-i0.005$
$\sigma_{sc}^k (cm^2)$ =	4.43×10^{-10}	2.68×10^{-10}
$\sigma_{sc}^x (cm^2)$ =	5.93×10^{-12}	3.59×10^{-12}
$\beta_{sc}^k (cm^{-1})$ =	1.63×10^{-13}	9.86×10^{-14}
$\beta_{sc}^x (cm^{-1})$ =	2.18×10^{-15}	1.32×10^{-15}

The important thing to note is that the volume scattering coefficients are more than an order of magnitude smaller than the volume extinction coefficients. For all practical purposes, then, extinction is equivalent to absorption for this particular case.

4. CLOUD LINE-OF-SIGHT TRANSMITTANCE

The transmittance (transmission loss) of the cloud along the axis of the radiometer beams can be approximated from the measured changes in brightness temperature, if it is assumed that no differences exist in the magnitude of the background brightness and cloud thermodynamic temperature. The first assumption was necessary because absolute radiation temperatures were not obtained. The second assumption is a simplifying assumption introduced for lack of information on the thermalization of the cloud.

At the time when the radiometers were first boresighted on the center of the cloud (T_o + 48 seconds) with their beams completely filled, the change in apparent temperature or transmission loss, ΔT_b, over the atmospheric background can be expressed as

$$\Delta T_b = T_{bb}t + T_{bc} - T_{bb} \qquad (9)$$

---

[2] Deirmendjian, D., "Complete Microwave Scattering and Extinction Properties of Polydispersed Cloud and Rain Elements," The Rand Corporation, Report R-422-PR, December 1963.

where

T_{bb} = apparent temperature of the background

t = cloud transmittance

T_{bc} = apparent temperature of the cloud

For computational purposes it was assumed that the apparent temperatures of the background at 10.2 and 30 GHz are 14 and 40°K, respectively (see Figure 7), and that the cloud was thermalized at 290°K.

A third assumption that scattered-in radiation is negligible compared to cloud self-emission was made. This assumption is a good approximation for optically thin clouds such as the one being considered, thus

$$T_{bc} = (1-t)\ T_c \tag{10}$$

where T_c is the thermodynamic temperature of the cloud. Equations (9) and (10) can be combined to give the following expression for transmittance:

$$t = 1 - \frac{\Delta T_b}{T_c - T_{bb}} \tag{11}$$

Substituting appropriate values in equation (11), the approximate cloud transmittances at each frequency are

$t^k = 0.946$

$t^x = 0.979$

To go one step further, substitution of these transmittances back into equation (10) yields the apparent temperatures of the cloud alone, from which insertion loss can be implied

$T^k_{bc} = 15.7°K$

$T^x_{bc} = 6.05°K$

The ratios of the cloud apparent temperatures is 2.6, which is somewhat less than the theoretical value of 2.94 (the ratio of the wavelengths) expected for Rayleigh particles, but with the assumptions employed no significance can be placed on this outcome.

These results will be useful for comparative purposes at a later point when similar results are derived from the computer models.

5. RAYLEIGH APPROXIMATIONS - EARLY PHASE

Any calculations of cloud properties at the early stages of its evolution will be truly speculative as supporting in-situ measurements are not available. Interpretation of radar data in terms of particle sizes and densities should yield some reasonable results. However, it is interesting to derive radiometric results independently from extrapolations of the aircraft particle sampling data.

a. The Dust Cloud at T_o + 48 Seconds

If the mass density from the period of 10 to 60 minutes after blast is linearly extrapolated back to the time T_o + 48 seconds, it is found that the mass density would have been approximately 30×10^{-8} gms cm^{-3} (see Figure 10). This is an increase of mass density by a factor of 44 over that at T_o + 11 minutes. While it is not reasonable to expect that the particle number density has increased by the same factor, as much of the mass at early times is made up of larger particles, it is not unreasonable to assume this to be the case just to estimate the effects of a mass increase where most particles remain in the Rayleigh size range. When this is done, the extinction coefficients as previously calculated for T_o + 11 minutes are just increased by a factor of 44. That is,

	$m = 1.88-i0.005$	$m = 1.63-i0.005$
$\beta_{ex}^{k}(cm^{-1}) \approx$	3.14×10^{-10}	3.84×10^{-10}
$\beta_{ex}^{x}(cm^{-1}) \approx$	1.07×10^{-10}	1.31×10^{-10}

From Figure 11 the cloud width at T_o + 48 seconds is found to be 1.0 km for which the optical thicknesses and corresponding transmittances are found to be

	$m = 1.88-i0.005$	$m = 1.63-i0.005$
$\tau^{k} \approx$	3.14×10^{-5}	3.84×10^{-5}
$\tau^{x} \approx$	1.07×10^{-5}	1.31×10^{-5}
$t^{k} \approx$	1	1
$t^{x} \approx$	1	1

These results indicate that the linear number density extrapolation alone will not produce the measured effects and that a much larger density would be required to give cloud apparent temperatures in the range of those op-

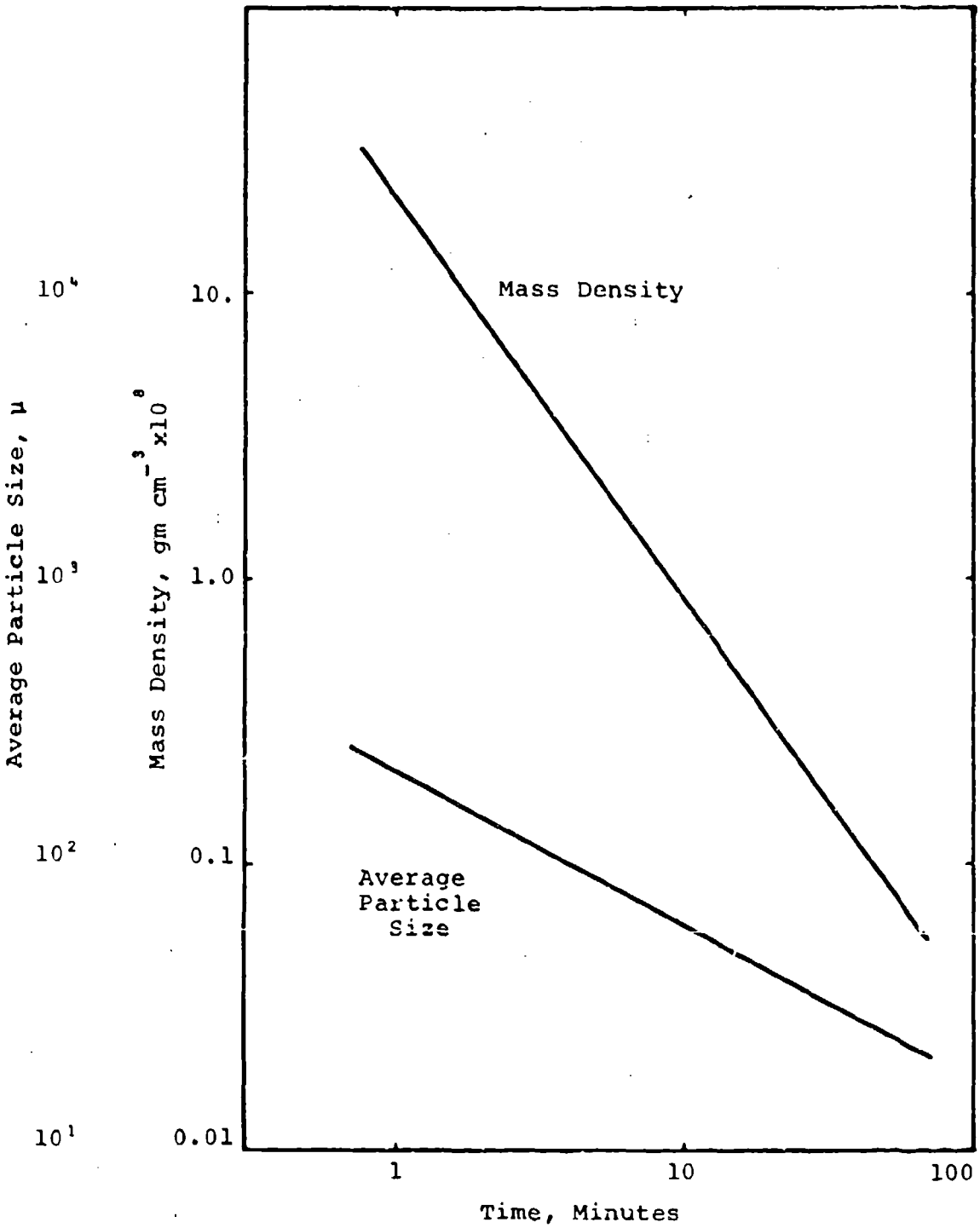

Figure 10 - Linear Extrapolation of Mass Density and Average Particle Size

(Data taken from DASA 2600 MR170 FR-948)

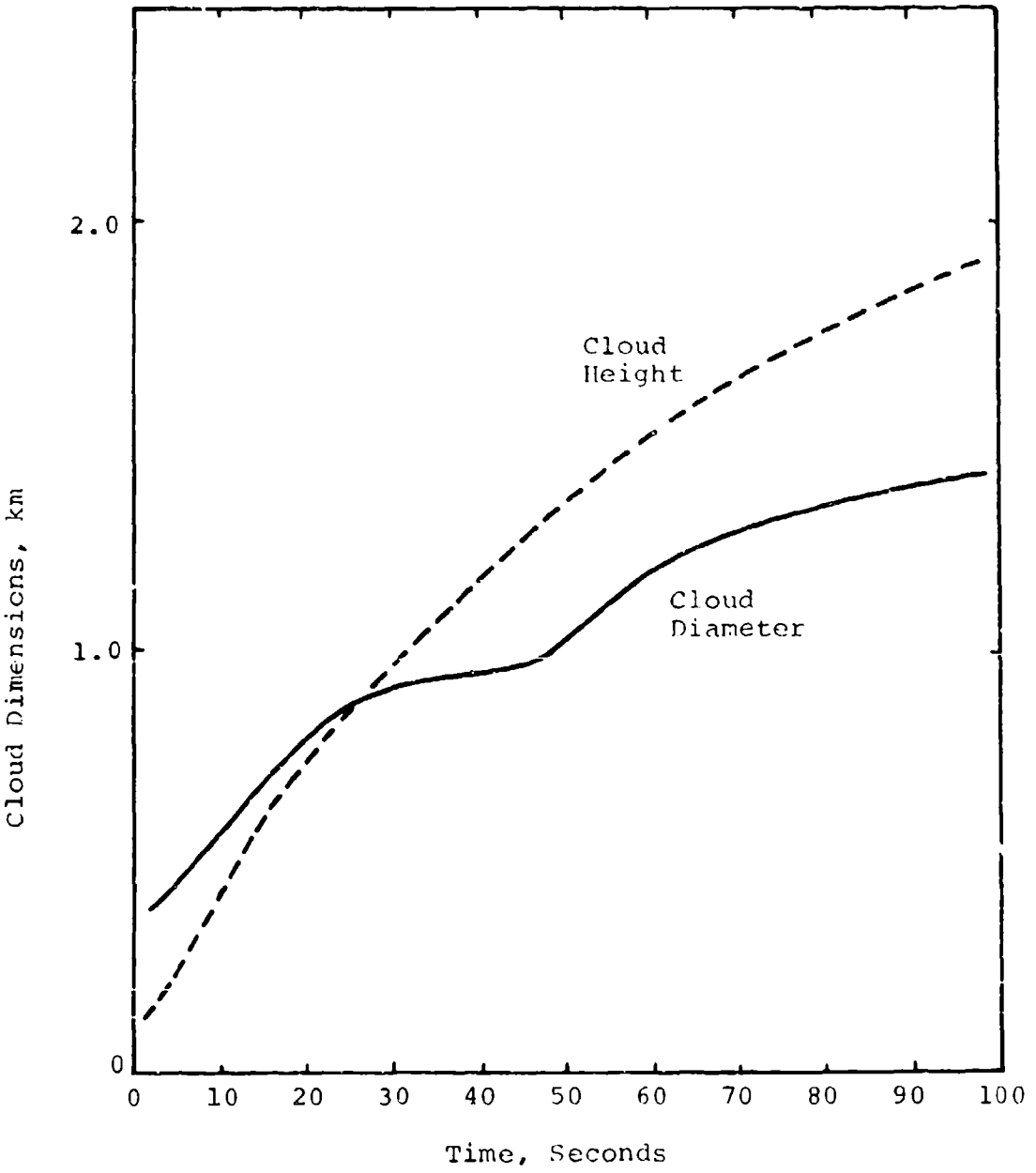

Figure 11 - Early Phase Cloud Dimensions

(Data taken from DASA 2600 MR170 FR-948)

served during Event Dial Pack. From the transmittance values it can readily be determined that a mass density over 1000 times higher would be necessary.

An additional increase in mass density by a factor of 1000 can be simply achieved by increasing the equivalent volume radius by a factor of 10. This would be r_e=510μ, still in the Rayleigh range, but of course an associated particle size distribution would have some particles in the Mie range. As r_e^3 enters into the expression for particle extinction cross section, equation (2), the factor of 1000 is realized. The values of extinction cross section, volume extinction coefficient, optical thickness and transmittance calculated for this new distribution are

	m = 1.88-i0.005	m = 1.63-i0.005
$\sigma_{ex}^k(cm^2)$ =	1.94×10^{-5}	2.37×10^{-5}
$\sigma_{ex}^x(cm^2)$ =	6.60×10^{-6}	8.06×10^{-6}
$\beta_{ex}^k(cm^{-1})$ =	3.14×10^{-7}	3.84×10^{-7}
$\beta_{ex}^x(cm^{-1})$ =	1.07×10^{-7}	1.31×10^{-7}
τ^k =	3.14×10^{-2}	3.84×10^{-2}
τ^x =	1.07×10^{-2}	1.31×10^{-2}
t^k =	0.969	0.962
t^x =	0.989	0.987

b. Absorption vs. Scattering

The relative values of absorption and scattering are dependent upon the dielectric properties of the particles as well as their size. If the absorption coefficients are an order of magnitude or greater than the scattering coefficients, then the emission of the cloud can be simply and directly calculated. On the other hand, if the scattering coefficients are of the same magnitude or greater than the absorption coefficients, then an iterative solution of the radiative transfer equations is called for. For this reason, it is essential to compare these coefficients for each particle distribution being considered.

Using equation (8) with a value of 737μ for r_{vv}, ten times that for the pass #1 distribution, the following volume scattering coefficients are obtained:

	m = 1.88-i0.005	m = 1.63-i0.005
$\beta_{sc}^{k}(cm^{-1})$ =	7.13×10^{-8}	4.31×10^{-8}
$\beta_{sc}^{x}(cm^{-1})$ =	9.55×10^{-10}	5.77×10^{-10}

From these values, the volume absorption coefficients are obtained by taking the difference of the volume extinction and scattering coefficients, in accordance with equation (7). The results are:

	m = 1.88-i0.005	m = 1.63-i0.005
$\beta_{ab}^{k}(cm^{-1})$ =	2.43×10^{-7}	3.41×10^{-7}
$\beta_{ab}^{x}(cm^{-1})$ =	1.06×10^{-7}	1.30×10^{-7}

The effects of wavelength, real part of the refractive index, and particle size are now apparent. At 1 cm the scattering coefficient is within an order of magnitude of the absorption coefficient for both values of refractive index, while at 3 cm, it is two orders of magnitude smaller. The large value of r_{vv}, with its corresponding value of x = 0.463 at one centimeter, has placed the particle distribution in the Rayleigh-Mie transition region. Note also, that for the larger value of refractive index, the ratios of absorption to scattering coefficients are lower than for the smaller value of refractive index. The significance of these results is that cloud emission can be accurately calculated in a straightforward manner only for the 3 cm case with the postulated particle distribution.

c. Cloud Albedo

Under the assumptions employed, the integrated albedo for single scattering, A, for the model cloud is given by

$$A = \frac{\beta_{sc}}{\beta_{ex}} \qquad (12)$$

so that at T_o + 11 minutes

	m = 1.88-i0.005	m = 1.63-i0.005
A^{k} =	2.29×10^{-2}	1.13×10^{-2}
A^{x} =	8.97×10^{-4}	4.52×10^{-4}

and at T_o + 48 seconds

	m = 1.68-i0.005	m = 1.63-i0.005
A^k =	2.27×10^{-1}	1.12×10^{-1}
A^x =	8.93×10^{-2}	4.4×10^{-2}

The integrated albedo provides another means of assessing both the emission and reflection properties of the cloud. For example, A ≥ 0.1 indicates that the complete radiative transfer problem, including scattering, absorption and emission, should be formulated to obtain correct results. The amount of energy from illuminating sources scattered by the cloud is dependent on source strength and the optical thickness and albedo of the cloud. Thus, while the magnitude of the albedo alone does not allow determination of the likelihood of measurable radar return from the cloud, the backscattering is directly proportional to albedo. Further considerations of radar backscattering are described in Paragraph 7.

d. Cloud Apparent Temperatures

It has been concluded, for the postulated dust particle distribution, that only at 3 cm can it be assumed that extinction is, for practical purposes, entirely by absorption. Then, at this wavelength, if it is further assumed that the cloud has thermalized at temperature T_c, the cloud apparent temperature, T_{bc}, would be given approximately by equation (10). Furthermore, letting the temperature of the cloud be 290°K, the cloud apparent temperature at 3 cm for cloud particles with the refractive index of fine sand (m=1.63-i0.005) is

$$T_{bc}^x = (1-.0987)\ 290 = 3.77°K$$

The total apparent temperature, T_b, viewing the cloud against the sky which has an apparent temperature, T_{bb}, is given by

$$T_b = T_{bb}t + T_{bc} \qquad (13)$$

while the change in apparent temperature from the sky background to occulted background is given by equation (9). For an elevation angle of 17° (zenith angle = 73°), the sky brightness would be approximately 14°K (see Figure 7). Taking this value as the average sky temperature for calculation purposes, the total apparent temperature and change in apparent temperature for the postulated dust cloud T_o + 48 seconds are:

$$T_b^x = 14(0.987) + 3.77 = 17.6°K$$

$$\Delta T_b^x = 3.77 - (0.013)14 = 3.59°K$$

This change in apparent temperature is close to that actually observed during Event Dial Pack, and with a slight increase in mass density the model could be made to match the value. However, without comparing the apparent temperature at a second wavelength and establishing a cloud scattering comparison (e.g., degree of polarization) an infinite number of particle distributions can be forced to satisfy this one criteria.

If the fact that the albedo at 1 cm is greater than 0.1 is ignored, and the apparent temperature and change in apparent temperature are calculated as though the transmittance were a measure of absorptive loss, the corresponding results are

$$T_b^k = 49.5°K$$

$$\Delta T_b^k = 9.5°K$$

The ratio of the changes in apparent temperature at the two wavelengths is 2.64 as compared with the observed ratio of 2.46. While this ratio is important, the accuracies of the record scalings and knowledge of which 30 GHz radiometer channel had improper gain enter into the measured ratio (i.e., if the H channel was assumed to be correct, the measured ratio would be 1.5).

The magnitudes of the preceding results are representative of those actually observed, and of course, the observations influenced certain assumptions. Besides the assumption that the Rayleigh mechanism holds and absorption dominates over scattering, these results are strongly affected by the choice of dielectric properties of the scatterers, their size distribution and their number density.

e. Discussion

The length and detail of the preceding analysis has been intended to convey the thought processes as well as the mechanics of arriving at a solution. This approach was taken because the observational data suggested that absorption (insertion loss) was the dominant process, i.e., the measured changes in apparent temperature caused by the dust cloud and their ratio at two wavelengths implied a Rayleigh mechanism. Starting with cloud particle data taken during the later phase of cloud evolution, an

approximate solution for an early stage was arrived at in two steps. This solution has a corresponding particle size distribution which has a significant number of particles in the Rayleigh-Mie transition region for 1 cm wavelength, and could therefore also produce a degree of polarization at this wavelength. It must be emphasized though that this solution is not unique.

Numerous assumptions were made throughout the analysis, many of them due to the lack of supporting data, but these assumptions had no drastic consequence because of the Rayleigh behavior of the real cloud. A general and complete solution which includes Mie theory and formulation of the radiative transfer problem would require supportive data in lieu of certain of these assumptions (such as homogeneity).

In the following sections the results of Mie calculations performed as a check on the preceding Rayleigh approximations and to extend the calculations to a wider variety of particle distributions and refractive index, are presented. The program assembled for these calculations will form the nucleus for development of a full general solution.

6. MIE THEORY CALCULATIONS

Even though the particle sizes for the later stage cloud satisfy the Rayleigh criterion, those in the earlier phase T_o + 48 seconds cloud may not. Therefore, full Mie theory calculations have been made, using a computer program for which the accuracy has been verified to particles of size parameter, x, greater than 5000. Analysis of the early phase cloud necessitates use of the program, while application to the later stage cloud provides useful checks on the Rayleigh approximations.

a. Description of Computer Routines

A computer program was written in FORTRAN IV to calculate the scattering and absorption properties of a homogeneous dust cloud made up of spherical particles with an arbitrary size distribution. The program is made up of several separate routines which will be briefly described here.

A routine written by Dave,[9] has been used to calculate

---

[9]Dave, J. V., "Subroutines for Computing Electromagnetic Radiation Scattering by a Sphere," IBM Scientific Center, Report 320-3237, May, 1968.

the Mie scattering parameters for each particle size in the dust cloud distribution. Included are the single particle efficiency factors for extinction and scattering, $Q_{ext}(r,m)$ and $Q_{sc}(r,m)$ from which the absorption efficiency factor is calculated by an analogous form of equation (7), i.e.,

$$Q_{ab} = Q_{ext} - Q_{sc} \tag{14}$$

In addition, four elements of the transformation matrix, Van de Hulst,[4] are determined as a function of scattering angle, and from these the intensity and degree of polarization of scattered radiation are calculated for a sphere illuminated by an unpolarized beam of radiation.

Once the scattering and extinction efficiencies have been found for each particle size in the cloud, the volume coefficients

$$\beta[n(r),m] = \pi \int_{r=o}^{\infty} r^2 n(r) Q(r,m) dr \tag{15}$$

are calculated for a given particle density distribution $n(r)$. In the program, analytical distributions are numerically integrated using Gauss-Legendre quadrature, tabular distributions are integrated using Lagrangian interpolation, and discrete distributions are numerically summed.

If the scattering is determined to be negligible ($\beta_{sc} << \beta_{bc}$) with respect to absorption, and assuming a homogeneous cloud, the apparent cloud temperature is calculated as in Paragraph 5.d. That is, the cloud optical thickness is calculated by equation (4), cloud transmittance by equation (5), cloud emission by equation (10) and the apparent temperature of the cloud by equation (13).

The program also provides other measures of the cloud, such as mass of particles per unit volume, equivalent volume radius and equivalent volume-squared radius for the given particle distribution.

b. Late Phase (T_o + 11 Minues) Cloud Results

Using the discrete distribution for pass #1, the scatter-

---

[4] Van de Hulst, H. C., "Light Scattering by Small Particles," John Wiley and Sons, Inc., 1957.

ing and brightness parameters were calculated for a dielectric constant of 2.3-i0.023 and for the coarse and fine sand dielectric constants, with imaginary parts of 0.001, 0.005, and 0.01. Table IV summarizes the results of that analysis.

c. Early Phase Cloud Model and Results

With the exception of the observed brightness temperature changes at T_o + 48 seconds, there is very little data from which a particle distribution at the early stage can be derived. Because of this lack of experimental information, another approach has been taken to formulate an early stage cloud model.

An analytical distribution often used to represent particulate clouds is the generalized gamma function[5]

$$n(r) = ar^{\alpha}\exp\{-br^{\gamma}\} \tag{16}$$

with

$$a = \gamma N \frac{b^{(\alpha+1)/\gamma}}{\Gamma(\frac{\alpha+1}{\gamma})}$$

$$b = \frac{\alpha}{\gamma} r_c^{-\gamma}$$

where r_c is the mode radius, and N is a density parameter. By varying the constants α and γ, this function can be made to fit many observed cloud particle distributions, over a large range of particle sizes. For the values of $r < r_c$, the shape of the distribution is determined primarily by the value of α, while that for $r > r_c$ is determined largely by γ.

Using the gamma function as an envelope for the discrete distribution of pass #1, the values of α = 1.2 and γ = 1.2 have been determined (Figure 12).

In formulating the early phase cloud, there is good reason to believe that only the density, and not the shape of the distribution for smaller particles will change from T_o + 48 seconds to T_o + 11 minutes. On the other hand, the shape of the distribution for larger particles will not yet be stable at T_o + 48 seconds, and will change as the larger particles settle out.

---

[5]Deirmendjian, D., "Complete Microwave Scattering and Extinction Properties of Polydispersed Cloud and Rain Elements," The Rand Corporation, Report R-422-PR, December 1963.

TABLE IV

LATE PHASE CLOUD RESULTS - COMPUTER MODEL

m	$\beta_{ex}(cm^{-1})$		$\beta_{sc}(cm^{-1})$		$\beta_{ab}(cm^{-1})$		Albedo	
	1 cm	2.94 cm	1 cm	2.94 cm	1 cm	2.94 cm	1 cm	2.94 cm
2.3 -i.023	2.35×10^{-11}	7.89×10^{-12}	2.27×10^{-13}	3.03×10^{-15}	2.39×10^{-11}	7.89×10^{-12}	9.6×10^{-3}	3.8×10^{-4}
1.87-i.01	1.46×10^{-11}	4.91×10^{-12}	1.35×10^{-13}	1.80×10^{-15}	1.45×10^{-11}	4.90×10^{-12}	9.2×10^{-3}	3.7×10^{-4}
1.63-i.01	1.76×10^{-11}	5.96×10^{-12}	8.28×10^{-14}	1.11×10^{-15}	1.75×10^{-11}	5.95×10^{-12}	4.7×10^{-3}	1.9×10^{-4}
1.87-i.005	7.36×10^{-12}	2.45×10^{-12}	1.35×10^{-13}	1.80×10^{-15}	7.23×10^{-12}	2.45×10^{-12}	1.8×10^{-2}	7.3×10^{-4}
1.63-i.005	8.85×10^{-12}	2.98×10^{-12}	8.28×10^{-14}	1.11×10^{-15}	8.77×10^{-12}	2.98×10^{-12}	9.2×10^{-3}	3.7×10^{-4}
1.87-i.001	1.58×10^{-12}	4.92×10^{-13}	1.35×10^{-13}	1.80×10^{-15}	1.45×10^{-12}	4.90×10^{-13}	8.5×10^{-3}	3.6×10^{-3}
1.63-i.001	1.84×10^{-12}	5.91×10^{-13}	8.28×10^{-14}	1.24×10^{-15}	1.75×10^{-12}	5.92×10^{-13}	4.5×10^{-2}	2.1×10^{-3}

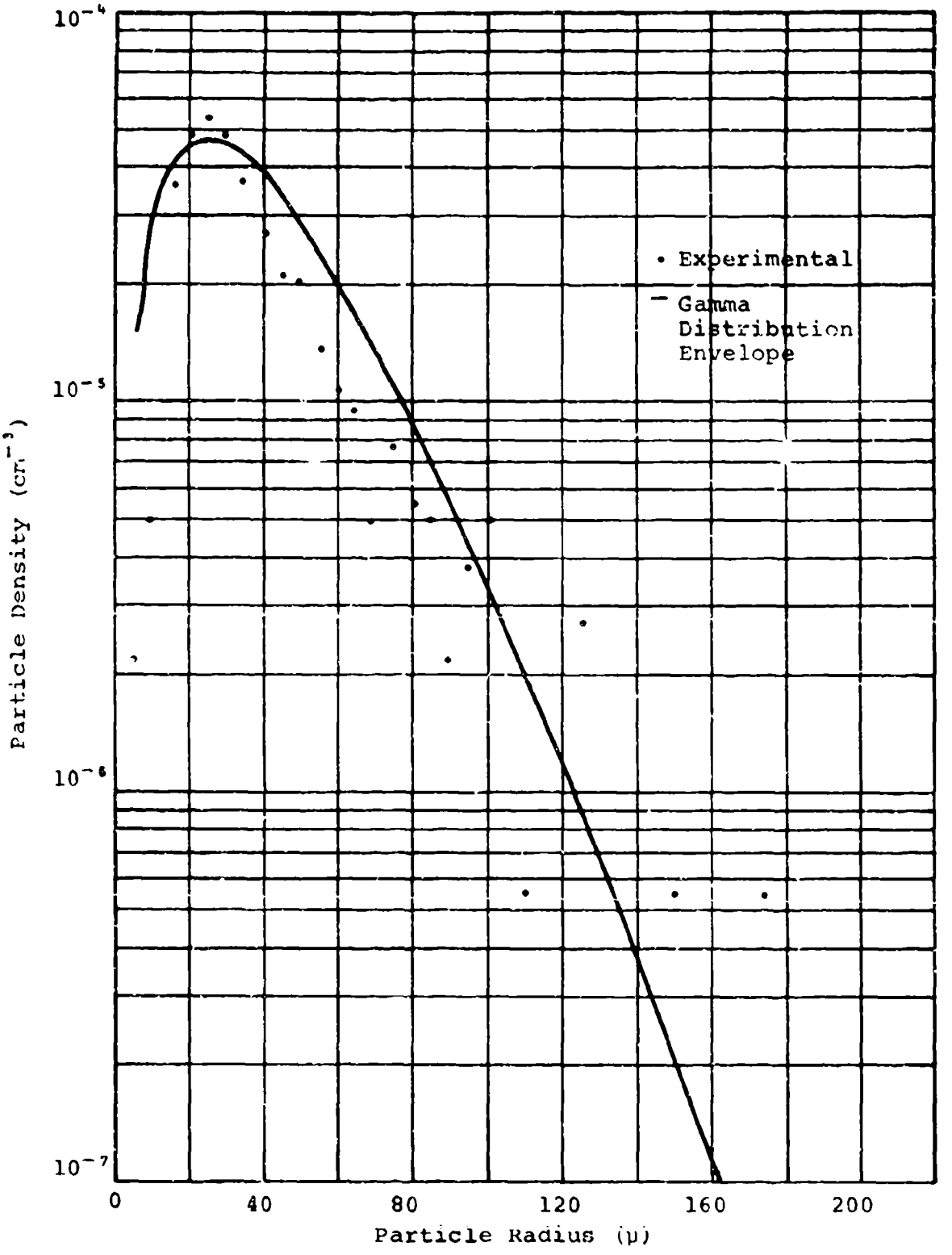

Figure 12 - Late Phase Cloud Distribution

With this in mind, the early phase cloud distribution was determined using an iterative process: α was held constant at 1.2, N and r_c were varied over a range of values consistent with the extrapolated mass and size data, (Figure 10), and γ was varied between 1 and 2. Figure 13 shows the distributions for four dielectric constants which give the changes in brightness temperature, T_b, from background to occulted, as shown in Table V. The corresponding volume coefficients are also shown in Table V.

Comparing the absorption and scattering coefficients at 1 cm, the albedo is greater than 0.1 in three cases, implying that the full radiative transfer equation should be solved to determine a more accurate brightness temperature. At 2.94 cm, the scattering coefficient is smaller than the extinction coefficient by at least an order of magnitude, and the selfemission temperature of the cloud as calculated is valid.

d. Comparison of Mie and Rayleigh Results

Excellent agreement can be seen between the volume scattering and extinction coefficients calculated for the late stage cloud model using the full Mie solution (Table IV), and those calculated using the Rayleigh approximations. In all cases, the approximation error is less than a few percent, and the assumption of an equivalent monodispersed medium with particles of an effective volume radius and volume-squared radius is certainly valid.

On the other hand, the early phase cloud particle size distribution model which has been used shows evidence that the scattering process is becoming non-Rayleigh. A measure of this departure from Rayleigh scattering is the ratio of extinction coefficients $\beta^k_{ex}/\beta^x_{ex}$. For the late phase cloud distribution

$$\beta^k_{ex}/\beta^x_{ex} \sim 2.98$$

The reason the ratio is somewhat greater than the expected value of 2.94 is probably due to the presence of the few large particles which approach the Rayleigh size limit. For the early phase cloud model distributions (Figure 13), the ratio has significantly increased to

$$\beta^k_{ex}/\beta^x_{ex} \sim 3.5$$

This is an expected result since, if the Mie process is predominate at the higher frequency, the extinction will be significantly larger than that predicted by the

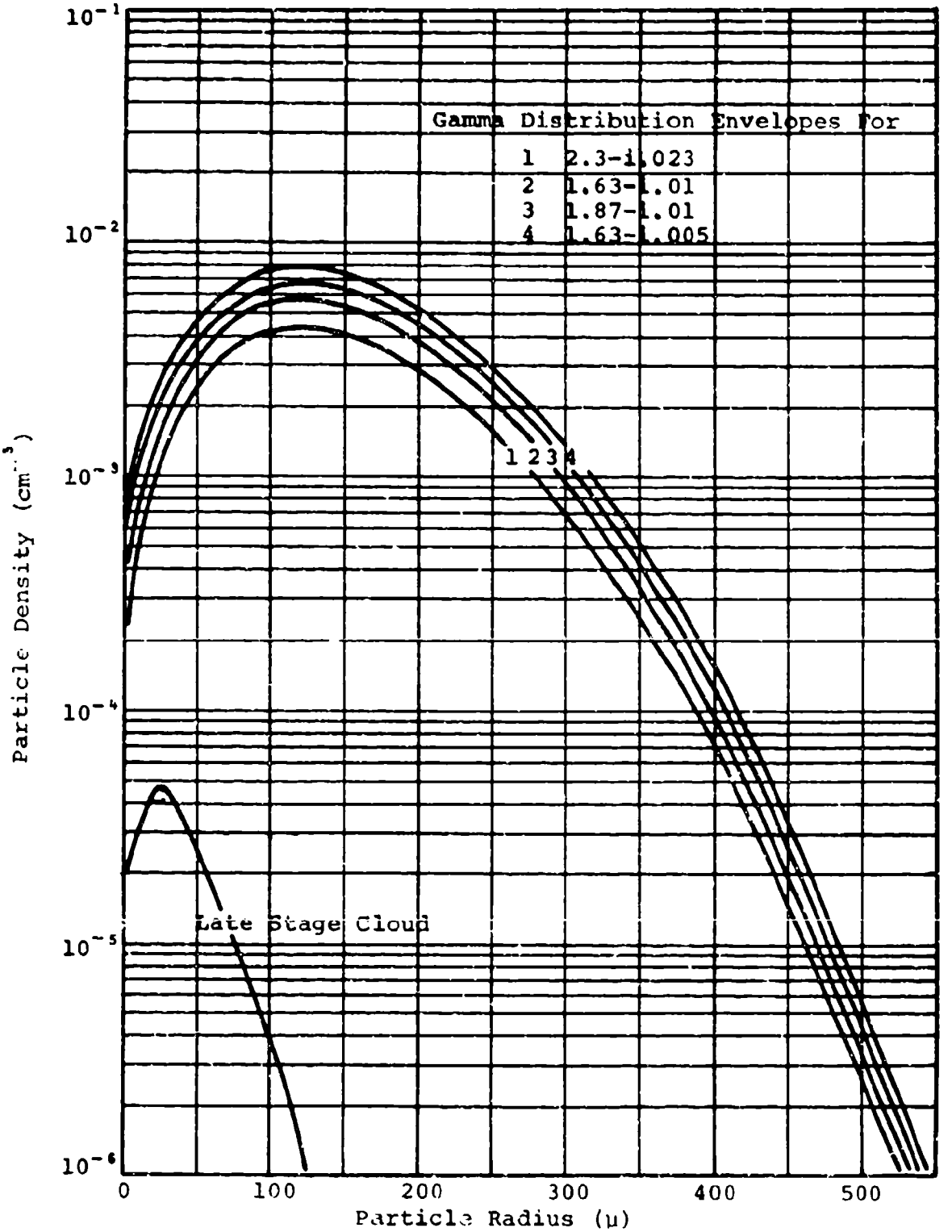

Figure 13 - Early Phase Cloud Distributions

TABLE Va

EARLY PHASE CLOUD RESULTS

m	Distribution (Figure 10)	ΔT_b (°K)		Albedo	
		1 cm	2.94 cm	1 cm	2.94 cm
2.3 -i.023	1	14.2	4.5	.15	.0074
1.63-i.01	2	13.3	4.6	.083	.0036
1.87-i.01	3	14.1	4.5	.15	.0071
1.63-i.005	4	12.9	4.2	.15	.0072

TABLE Vb

EARLY PHASE CLOUD VOLUME COEFFICIENTS

m	$\beta_{ex}(cm^{-1})$		$\beta_{sc}(cm^{-1})$		$\beta_{ab}(cm^{-1})$	
	1 cm	2.94 cm	1 cm	2.94 cm	1 cm	2.94 cm
2.3 -i.023	5.86×10^{-7}	1.64×10^{-7}	9.22×10^{-8}	1.21×10^{-9}	4.94×10^{-7}	1.62×10^{-7}
1.63-i.01	5.48×10^{-7}	1.69×10^{-7}	4.56×10^{-8}	6.07×10^{-10}	5.03×10^{-7}	1.68×10^{-7}
1.87-i.01	5.81×10^{-7}	1.65×10^{-7}	8.85×10^{-8}	1.17×10^{-9}	4.93×10^{-7}	1.64×10^{-7}
1.63-i.005	5.35×10^{-7}	1.55×10^{-7}	8.22×10^{-9}	1.11×10^{-9}	4.53×10^{-7}	1.54×10^{-7}

Rayleigh approximations.

Similar analysis using the absorption coefficients for the later phase cloud shows that

$$\beta^{k}_{ab}\ \beta^{x}_{ab} \sim 2.95$$

whereas the early stage distributions all yield

$$\beta^{k}_{ab}\ \beta^{x}_{ab} \sim 3.05$$

This is further evidence of the non-Rayleigh nature of the cloud.

Viewing these results, it is now apparent that the ratio of 2.64 found in Paragraph 5.d for the ratio of the changes in apparent temperature at 1 cm and 3 cm is low for the reason that the Rayleigh approximations are in error for particles (r_e, r_{vv}) which violates the Rayleigh criteria $x < 0.1$. At the same time, the question as to why the ratio obtained from the Event Dial Pack measurements was even lower is raised. The answer is not clear, but the alternatives are calibration errors or properties of the dust cloud not accounted for (e.g., scattering or structure).

e. Columnar Dust Content

The quantity of layered sand required to cause comparable increases in the 30 GHz apparent temperatures of the zenith sky to those observed on the Event Dial Pack cloud are 0.387 gm cm^{-2} and 1.06 gm cm^{-2} for coarse and fine sand, respectively, (see Figure 8). The approximate values obtained from the computer models are found by dividing the mass of particles per unit volume by the particle equivalent volume per unit volume. The results for coarse and fine sand are 25 gm cm^{-2} and 27 gm cm^{-2}, respectively. These results are tractable because bulk material attenuates more than the same material in suspension. Furthermore, the ratio of bulk extinction to particulate extinction in the Rayleigh region can be several orders of magnitude. This ratio for the same material at wavelengths that place the particulates in the Mie region can approach unity. Therefore, for particle size distributions in the Rayleigh-Mie transition region, an order of magnitude seems reasonable.

7. RADAR BACKSCATTER

The radar return from the dust cloud can be calculated using:

$$P_r = \frac{P_t A_e^2 \theta \phi \ell}{72 \lambda^2 R^2} \beta_{sc} \exp(-2\beta_{ex} L) \qquad (17)$$

where:

$P_{r,t}$ = received (backscattered) and transmitted powers

A_e = antenna apertural area

θ, ϕ = horizontal and vertical antenna bandwidths

ℓ = radar pulse length

R = range to the centroid of the scattering volume

β_{sc} = volume scattering coefficient of the cloud

L = range to the centroid of the scattering volume from the leading edge of the cloud

The following characteristics of the LAPQ-1 radar, used in the Event Dial Pack, are known:

Peak power = 100 kw

Wavelength = .858 cm

Pulse length = 1 sec

Minimum detectable signal =-101 db

Antenna gain = 47 db

Antenna beamwidth = 0.75 degrees

Applying equation (17) for a radar range of 3000 m, the approximate radar return from the dust cloud is given by

$$P_r = .92 \beta_{sc} \qquad (18)$$

Evaluating this equation for a cloud with particle refractive index:

$$m = 1.63 - i0.01$$

and the volume scattering coefficients corresponding to the late phase cloud data, and the postulated early phase cloud model (Paragraph 6.c);

$$\beta_{sc} \begin{cases} 1.53\times10^{-19}\ cm^{-1};\ T_o + 11\ minutes \\ 8.44\times10^{-8}\ cm^{-1};\ T_o + 48\ seconds \end{cases}$$

the radar returns are:

$$P_r = 1.41\times10^{-19}\ watts;\ T_o + 11\ minutes$$

which is approximately -98 dbm during the dust cloud dissipation phase, and

$$P_r = 7.76\times10^{-8}\ watts;\ T_o + 48\ seconds$$

or approximately -41 dbm during the growth phase. This indicates that for an LAPQ-1 type radar, the cloud should be readily detectable past T_o + 11 minutes. One factor not taken into account is a possible change of radar range as the cloud drifts from ground zero. A range increase of 10 times (i.e., R = 30,000 m) would have made the cloud undetectable at T_o + 11 minutes.

For a radar operating at 3 cm with the LAPQ-1 system characteristics, the radar return is given by

$$P_r = 10.1\ \beta_{sc} \qquad (19)$$

With a particle refractive index m = 1.63-i.01, the scattering coefficients are:

$$\beta_{sc} \begin{cases} 1.11\times10^{-15}\ cm^{-1};\ T_o + 11\ minutes \\ 6.07\times10^{-10}\ cm^{-1};\ T_o + 48\ seconds \end{cases}$$

The radar returns are then

$$P_r = 1.12\times10^{-14}\ watts;\ T_o + 11\ minutes$$

or about -109 dbm for the late stage cloud, and

$$P_r = 6.12\times10^{-9}\ watts;\ T_o + 48\ seconds$$

or about -52 dbm. The early phase cloud is still readily detectable, while the late stage cloud would probably not be seen.

8. POLARIZATION CONSIDERATIONS

The approximate methods used in the analysis up to this point tacitly assume a spherical homogeneous cloud composed of spherical particles. If it is additionally assumed that single scattering governed by the Rayleigh laws applies, and that the cloud is optically thin, polarized emission would not be observed. Even if the particles were non-spherical, their random orientation in the cloud should eliminate any polarized emission.

Since the cloud was non-homogeneous and not spherical, it is possible to imagine a situation in which, although the cloud is optically thin, the radiometer could be viewing stratification within the cloud at near grazing angles. Depending on the structure and the density gradients which the radiometer is viewing, some polarized emission could be observed. However, such an occurance would be evidenced by an irregular brightness curve, as the cloud passed through the radiometer beam, while the Event Dial Pack record is relatively smooth. This leaves the most likely source of polarized energy, if observed, the scattering of radiation which illuminates the cloud.

The sources of cloud illumination to be considered are the sun, the atmosphere, and the ground, since the radars used to probe the cloud have been treated separately in Paragraph 7. Polarized or unpolarized illuminating radiation can give rise to measured polirization if the source strengths are sufficient for the scattered energy to be detectable. Highly polarized incident radiation will in general be somewhat depolarized, while unpolarized incident energy will exhibit some degree of polarization when scattered from a cloud such as is being discussed here.

The direct sun is the easiest case to treat, and its treatment will give some insight to the problem. At 1 cm wavelength the sun can be thought of as a distant point source with a brightness temperature of about 7000°K. Referring to Figure 6, which shows the experiment geometry, it is seen that the half power radiometer beam defines an approximately cylindrical volume within the cloud. The particles contained in this volume are assumed to be the only active scatterers. The dimensions of the cylinder are 1000m length (the width of the cloud at T_o + 48 seconds) by 113m mean diameter.

To determine if scattered solar radiation could contribute to the measured brightness of the dust cloud, a best possible case is considered. Let the scattering angle be 90 degrees so that all elements of the scattering phase matrix are zero except P_1. The power density of the solar radiation, S, incident on the dust cloud at 1 cm wavelength is of the order of 10^{-25} watts $cm^{-2}Hz^{-1}$. Under the single scattering assumption, each cubic centimeter of the cylindrical volume will be illuminated by radiation of this intensity, and each will scatter an amount $1/2\beta_{sc}P_1S$ toward the radiometer (ignoring extinction of the incident or scattered power by the cloud). The power density of the scattered solar flux, S^s, at the radiometer is

$$S^s = 1/2 \frac{\beta_{sc} P_1 SV}{4\pi R^2} \qquad (20)$$

where V is the volume of the scattering cylinder and R is the range of the radiometer from the centroid of the cloud. Evalua-

ting equation (20) at T_o + 48 seconds and λ = 1 cm for the postulated early phase cloud particle distribution (see Paragraph 6.b) with refractive index m = 1.63-i0.01 and $\beta_{sc} = 4.56 \times 10^{-8}$ cm^{-1} (see Paragraph 6.b), gives

$$S^s = 3.74 \times 10^{-32} \text{ watts cm}^{-2} \text{ Hz}^{-1}$$

The power density at the radiometer corresponding to the apparent temperature of the cloud is given by

$$S_c = \frac{2\pi k T_b}{\lambda^2} \left(\frac{r}{R}\right)^2 \qquad (21)$$

where r is the radius of the scattering cylinder defined by the antenna beamwidth, and k is Boltzmann's constant. Evaluation of this equation gives

$$S_c = 1.31 \times 10^{-24} \text{ watts cm}^{-2} \text{ Hz}^{-1}$$

which is eight orders of magnitude greater than the scattered solar flux. Therefore, it can be concluded that scattered solar energy can be of no consequence.

Consideration of radiation from the ground is somewhat more complicated. To make the analysis tractable, the ground is treated as an idealized plane Lambertian surface of uniform temperature, T_e. The power density of the radiation from the ground at the centroid of the cloud is approximately

$$S_e \cong \frac{2\pi k T_e}{\lambda^2} \qquad (22)$$

where it has been assumed that the effective surface is contained in a solid angel of π steradians as a consequence of the Lambertian properties of the ground. Evaluation of the equation (22) for a surface temperature of 300°K gives

$$S_e = 2.60 \times 10^{-20} \text{ watts cm}^{-2} \text{ Hz}^{-1}$$

which yields the corresponding power density at the radiometer:

$$S_e^s < 6.48 \times 10^{-27} \text{ watts cm}^{-2} \text{ Hz}^{-1}$$

Note that this value has been explicitly stated as "less than" because of numerous optimum assumptions. Comparing this value with the power density corresponding to the cloud apparent temperature, it is seen to be more than two orders of magnitude smaller. This leaves the terrestrial radiation scattered by the cloud at the detection threshold of the radiometer, with negligible contribution to the total signal.

Atmospheric radiation presents a similarly difficult radia-

tive problem, in which the cloud is immersed in the source. However, the radiation temperature of the atmosphere averaged over 4π steradians is less than 100°K at 1 cm, which produces a scattered power density at the radiometer of about the same level as the terrestrial radiation. Therefore, it can be concluded that radiation from the atmosphere can also be neglected.

The treatment of these various sources was based on the selection of one particle size distribution that led to reasonable agreement with observations. While this does not allow unique assessment of the cloud emission and scattering, the results seem to be compatible with the limited data available.

SECTION III

SUMMARY, CONCLUSIONS AND RECOMMENDATIONS

In the preceding analyses, the problem of microwave emission and scattering by a tenuous cloud of earth debris (called dust throughout the report) has been considered in an approximate way. First, using debris sample data acquired with an airborne particle sampler and particle refractive index values the volume extinction, scattering and absorption coefficients were calculated by Rayleigh formulas. In addition, optical thickness, transmittance and cloud albedo were calculated. Second, an extrapolation to an early time (T_o + 48 seconds) was made by increasing the mass density by a factor of 4.4×10^4 times. Again, the radiation transfer parameters were calculated by the Rayleigh approximations. This extrapolation led to cloud transmittances and cloud brightness temperatures close to those actually observed by the 10.2 and 30 GHz radiometers during Event Dial Pack.

As a check on the Rayleigh results and to extend the calculations to a wider range of particle size distributions and refractive indices, a computer program was written utilizing generalized Mie scattering routines. With a version of this program, the validity of the Rayleigh approximations for the late stage (T_o + 11 minutes) cloud was determined. In addition, a dust cloud particle distribution model was postulated, and using this, a combination of mass density, particle density and refractive index were iteratively selected to yield results close to the actual observations of the early stage (T_o + 48 seconds) cloud.

Considerations of radar detectability using computed values of Mie scattering coefficients suggest that the cloud should have been readily detectable in its early stages by both 3 and 0.86 cm radars, and therefore information about its structure could be determined by such means. In the later phase of cloud evolution, $T > T_o$ + 11 minutes, the cloud should still have been giving a usable return of 0.86 cm but not at 3 cm. It is not known whether this is the case, but the unique determination of early phase cloud properties hinges on this type of data.

Using the same model as was used to assess radar return, the scattering of radiation from the sun, ground and atmosphere toward the radiometers was treated. None of these sources was found to contribute measurable amounts of radiation, and therefore do not contribute any significant polarized energy for the postulated early stage cloud model.

The conclusions of this report are as follows:

1. The late phase cloud, $T > T_o$ + 11 minutes, would have been transparent to the 10.2 and 30 GHz radiometers.

2. There are many models which approximately predict the observed apparent temperatures of the early phase cloud (T_o + 48 seconds).

3. The controlled measurements data show that polarization was insignificant. The derived models are consistent with this conclusion.

4. Approximately 25 gm cm^{-2} of debris was required to cause the observed increases in apparent temperature.

5. Strong radar returns should have been observed at 0.86 and 3 cm from the early phase cloud, but the late phase cloud should have been marginally detectable only at 0.86 cm.

6. Insertion loss and transmission loss cannot be absolutely calculated because of cloud backgrounds and change in cloud thermal temperature, cloud transmittance is a better descriptive property.

If reliable polarization and radar backscatter data had been available, it would have been possible to derive a unique model of a homogeneous spherical debris cloud. To handle a structured cloud or one in which scattering was an important process would have required formulation of the radiative transfer problem, a task beyond the scope of this study. As a spherical, homogeneous cloud was assumed, the complete scattering by the cloud would be given classical scattering patterns.

The value of the radiometers in experiments such as Event Dial Pack should not be underestimated, for they provide information complementary to that obtained by radar techniques. Interpretation of these two types of data jointly should provide details on the structure of such a cloud, as well as properties of the particles of which it is composed. Whereas a radar can supply scattering and extinction data, a radiometer can supply absorption and extinction data, which together completely define the radiative properties of the cloud. It is therefore recommended for future experiments of this type, that

1. Three radiometers, one each at wavelengths of 3, 1.25 and 1 cm, be installed at the test location. The 1.25 radiometer would be used to provide data on water vapor and cloud thermalization as well as providing an additional constraint for iterative solution.

2. These radiometers should be absolutely calibrated to give the total apparent temperature as well as the change in apparent temperature

3. These radiometers should have the capability of scanning

whenever the cloud has dimensions large compared with the radiometer beamwidth.

4. These radiometers should track the cloud as it ascends and then drifts from ground zero.

5. Synchronizing information between radar positioning and radiometer positioning be recorded for analysis purposes.

In addition to the refined radiometric systems, a complete general computer program which includes the radiation transfer formulation for an arbitrarily shaped cloud should be developed. Some of the basic elements for such a computer model are already available, including the scattering routines utilized in this study and radiation transfer models utilized in paststudies. With a complete model available, coordination among experimenters and proper data recording and handling could assure rapid accomplishment of the dust cloud analysis.